Applied Geochemistry 202 (2026) 106784

Contents lists available at ScienceDirect

Applied Geochemistry

journal homepage: www.elsevier.com/locate/apgeochem

# Application of the stratigraphy-controlled geochemical data analysis in mineral prospective mapping in glaciated terrain

C. Kalubowila *, M. Raatikainen, P. Sarala

*University of Oulu, Oulu Mining School, P.O. Box 3000, Oulu, 90014, Finland*

ARTICLE INFO

Editorial handling by: Dr. O.P. Kreuzer

*Keywords:*
Mineral exploration
Glacigenic sediments
Till geochemistry
Compositional data
Gold
Orthomagmatic mineralization

ABSTRACT

Till is a preferred geochemical sampling medium for mineral exploration in glaciated terrains due to its good indication of local or regional bedrock composition and secondary, down-ice transportation. However, the influence of till stratigraphy on the detection of subsurface mineral deposits remains rarely investigated. This is particularly important in areas having thick glaciogenic sedimentary cover with several glaciation phases. We demonstrate this complexity in Finnish Lapland, where the glacial sediment cover is thick and composed of several till units which represent separate glaciations during the Quaternary. The average glacial sediment drape thickness in Lapland is 5.5 m, although in places it can be several tens of meters. Two approaches were applied to study till stratigraphy based on the till geochemistry: a) a fixed depth interval method, and b) a statistical approach method. The fixed, 1-m depth interval method was used to divide till layers based on geochemical composition from the ground surface to the bedrock surface, while the statistical approach analyses changes in elemental content with depth by identifying optimal depth intervals in till geochemistry. Fuzzy overlay maps were generated for two study areas concerning different depth intervals identified by the described methodologies. Results indicate that the optimal depth range for detecting gold mineralization in the selected sub area 1 in Kittilä is 1.7–3.6 m, whereas the optimal depth for detecting orthomagmatic deposits in the selected sub area 2 in Akanvaara is 2.8–5.2 m. The statistical till depth profiling improves the predicted maps for specific mineral deposits compared to the fixed depth intervals, and it can enhance the reliability of mineral deposit detection during exploration in glaciated terrains.

## 1. Introduction

Demand for mineral resources is increasing due to the continuous rise in global population and living standards. Also, environmental issues, social impacts, and costs associated with mining activities have a great effect on finding new natural resources (Rasilainen et al., 2010, 2012). Finding new ore deposits requires active exploration, which is seen globally as a strong business with a total budget of about 12.5 billion U.S. dollars per year (S&P global market intelligence, 2024). Mineral exploration also covers large areas in the Northern Hemisphere, which are dominantly covered by glacigenic sediments. Sediments were deposited by numerous glaciations during the Quaternary period. For example, during the Pleistocene glacial maximum, the majority of North America and Europe were covered by ice sheets, where in Europe only 200 km ice free corridor was left between the Nordic and Alpine piedmont glaciers (Ehlers and Gibbard, 2007). In addition, during the Last Glacial Maximum (LGM), around 34.5 million km$^2$ of the northern region was under ice (Lindgren et al., 2016). For that reason, till and other glaciogenic sediments are the dominant soil type in Canada, Iceland, Fennoscandia, the northern parts of Central Europe and in significant areas of Ireland, the United Kingdom, the United States and Russia (Shilts, 1976; McClenaghan and Paulen, 2018).

Till is the sediment that was eroded, transported and deposited by moving glaciers, and particularly during the retreat, i.e., deglaciation phase of glaciation. Till, as a dispersed material, represents the composition of the underlying bedrock within a range of distances from the sources or source areas. Therefore, it is essential to study glacigenic landforms, ice-flow indicators such as till fabric and striae, till stratigraphy and composition for understanding glaciers' glaciodynamics and depositional conditions in the study areas (Sarala, 2015). Till geochemistry is a commonly used technique and effective tool in studying element concentrations and distribution in glaciated terrains on different scales. It has been successfully used for 60-70 years as a basic tool in mineral exploration (McClenaghan et al., 2023). For

* Corresponding author.
*E-mail address:* charmee.kalubowila@oulu.fi (C. Kalubowila).

https://doi.org/10.1016/j.apgeochem.2026.106784
Received 30 October 2025; Received in revised form 3 March 2026; Accepted 18 March 2026
Available online 19 March 2026

example, regional till geochemical data collected by the Geological Survey of Finland (GTK) in 1982–1991 with a sample density of 1 sample per 4 km$^2$ (including 82 062 samples) (Gustavsson et al., 1994; Salminen, 1995) has been used in mineral exploration in Finland since the end of the 1980's (Salminen and Tarvainen, 1995; Sarala, 2015). There is also another regional till geochemical data available in Finland, the targeting till geochemical dataset. It was also collected by GTK in 1971–1983 as sampling lines at intervals of 1–2 km and at point intervals of approximately 100-400 m (Gustavsson et al., 1979). This data is freely available online on the website of GTK (Geological Survey of Finland, 2015). It covers selected parts of northern Finland and the Ladoga-Bothnian Bay zone (GTK, 2024). The data contains 385 000 samples, and the sampling density is 6–12 samples per km$^2$ (Gustavsson et al., 1979). The sampling depth varies between 0.1 and 25.3 m, and the average sampling depth is about 2 m (Kalubowila et al., 2025). The concentration of 17 elements was analysed using emission quantometer EKV (Danielsson et al., 1959; Danielsson and Sundkvist, 1959a;b). Although this dataset has received limited attention and has been little used in mineral exploration in the past, it has recently started to be analysed (Taivalkoski, 2017; Puchhammer et al., 2024; Kalubowila et al., 2025; Raatikainen et al., 2025). Which is why it is the focus of this research. The underutilisation of the data set in earlier years might be due to limited confidence in the analytical method that used the emission quantometer (EKV) to measure element concentrations and its prevailing data quality issues, such as levelling problems between adjacent map sheets. In addition, the targeting till dataset comprises concentrations at different depths for each sampling point. It provides the possibility of so-called stratigraphy-controlled till geochemical data analyses (Sarala, 2015), which is also an underused technique in mineral exploration. Element concentrations in different till units can be used in estimating source areas for each layer, as well as revealing sub-outcropping mineralization or even deep-seated, hidden mineral deposits. Therefore, it is important to determine the most favourable depth range of the till profile for generating predictive maps and to identify the optimal depth range that contains the geochemical signal of a particular mineralization.

In this paper, we utilized archived till geochemical data from a couple of study areas from northern Finland to illustrate the effectiveness of different data analytical techniques. The study areas are located in the central part of northern Finland (also called Central Lapland), where two sub-areas were selected to test the predictions for gold (sub-area 1 in Kittilä) and orthomagmatic deposits (sub-area 2 in Akanvaara). Two separate methods were used to study the till profile: the fixed depth interval method and the statistical approach method. Fixed depth interval method focused on the till layers based on 1 m depth interval. In the statistical approach method, concentration changes in selected elements were detected and suitable till depth intervals were recognized to identify the optimal depth range for detecting different types of mineral deposits. Fuzzy overlay maps were generated for each depth interval identified by two separate methods in the individual study areas and were validated using a receiver operating characteristic curves (ROC) and prediction area (P–A) plots.

## 2. Study area

### 2.1. Central Lapland

The two study areas, 1 (Kittilä) and 2 (Akanvaara) (Fig. 1), are located in the Central Lapland, a subregion of northern Finland. They lie within the central Lapland belt, which extends into northern Norway,

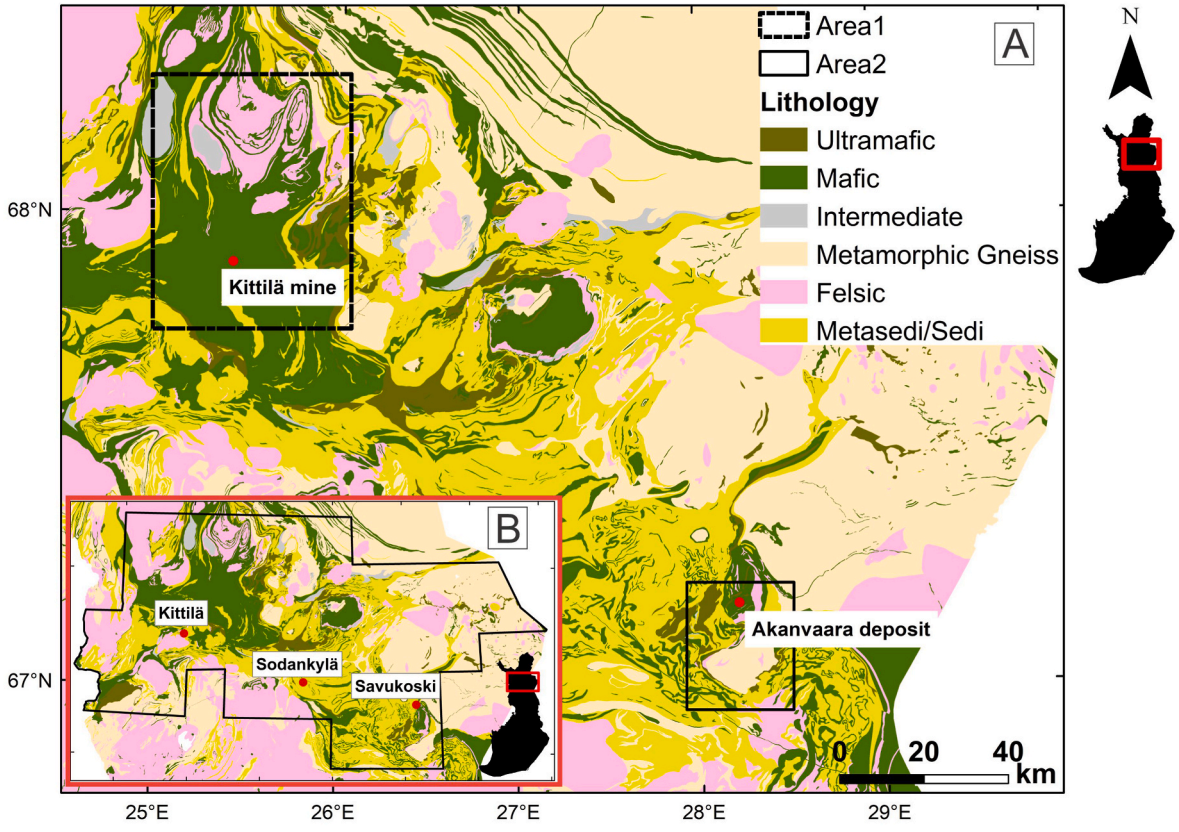


**Fig. 1.** Simplified compositional grouping of bedrock units together with sedimentary and metasedimentary units (Metasedi/Sedi) in (A) study areas 1 and 2 (B) the location of sampling points used for the targeting till geochemical data. The bedrock map is constructed using digital map information from the GTK Maankamara: http://gtkdata.gtk.fi/Maankamara/index.html © Geological Survey of Finland (2015, GTK Basic license version 1.1), Bedrock of Finland 1:200000 (2023–2024), CC-BY-4.0.

Sweden and Russian Karelia. The central Lapland belt overlies the Archean Karelian craton, and it includes several areas dominated by either volcanic or sedimentary rocks (Patten et al., 2023). Moreover, according to Hanski and Huhma (2005), the central Lapland belt records a long and complex tectonic history of more than 500 Ma during the Svecofennian orogeny with deformation, thrusting and shear zones. It was affected by the Svecofennian collision to the southwest and by thrusting of the Lapland granulite belt from the northeast, acting as a foreland fold and thrust belt between two opposing collisional systems. Later, some notable shear zones such as the Sirkka-line at the southern margin of the Kittilä greenstone area and Kolari shear zone, near the Finnish-Swedish border, were created (Hanski and Huhma, 2005). The selected study area hosts important geological formations, including the greenstone belt (central Lapland belt), layered and mafic intrusions with numerous mineral deposits.

### 2.2. Surficial geology

Central Lapland has been subject to multiple glaciation events throughout the Quaternary. The latest of these glaciation events is known within northern Europe as the Weichselian glaciation, which had three distinct stages: early, middle and late (Johansson et al., 2011). For most of the glacial period, the Weichselian ice divide zone has been on top of central Lapland. This has led to preservation of older sediments (Hirvas, 1991). Furthermore, the ice divide zone, being in central Lapland multiple times, has also preserved the underlying preglacial weathered bedrock. There is no definitive age defined for this weathered bedrock surface. The possible age for weathering has been proposed to have begun from around 541 Ma to somewhere around 25 Ma (Hyyppä, 1983; Hirvas, 1991; Johansson and Kujansuu, 2005). According to Hirvas (1991), the transport distance for till debris is short as the movement of the bottom of the glacier is minimal within the ice divide zone. According to Hirvas (1991), some of the till within the study area can be described as weathered bedrock till, an indication that the till is derived directly from the local underlying weathered bedrock. Sometimes, weathered bedrock till is difficult to distinguish from weathered bedrock.

### 2.3. Till stratigraphy

Hirvas (1991) studied the Pleistocene stratigraphy of Finnish Lapland based on the flow stages of the continental ice sheet or glacial stages comprehensively. According to this, 6 distinct ice flow or glaciation phases have been identified in Finnish Lapland, each corresponding to till beds (Bed I – VI) ranging from youngest to oldest. The topmost till bed (I) was deposited during the latest stage of deglaciation, whereas the common thickness ranges from 1 to 1.5 m (average 1.3 m) (Hirvas, 1991; Johansson et al., 2011). However, bed I is not continuous in Lapland, as in some pits it was not recognized. Till bed II was deposited during the youngest glacial flow stage and the mean thickness of this layer in the ice divide zone is 1.9 m, north of it is 2.5 m and south of it is 2.6 m (Hirvas, 1991). However, the thickness of till bed III could not be determined with certainty and recorded thicknesses range from less than 0.5 m to over 6 m (Hirvas, 1991). Till beds that are older than till bed III were identified in several study areas and those till beds are collectively referred to as older till beds. Their origin is not clear, as some of the structural features may have been wiped out due to glacier loading, weathering, or overprinted by younger glacial flows. Moreover, the thicknesses of older till beds are uncertain, where the recorded values range from 1 m to 6.4 m. The average depth of till beds within Lapland is 5.5 m (Mäkinen, 1975). In some cases, the older beds (IV–VI) have been re-evaluated after dating studies using the optically stimulated luminescence (OSL) method showed that the underlying and overlying sand and silt deposits were aged Eemian or younger (Sarala, 2011, 2014; Lunkka et al., 2015; Putkinen et al., 2020).

### 2.4. Bedrock geology

The study area is located within the central Lapland belt. The central Lapland belt consists of Paleoproterozoic supracrustal rocks, with mafic to ultramafic intrusions. Felsic and lamprophyric rocks, as well as syn-orogenic and post-orogenic granitoids, are also affiliated with the central Lapland belt. The central Lapland belt has been divided by Köykkä et al. (2019) into six groups; from oldest to youngest, these groups are the Salla group, the Kuusamo group, the Sodankylä group, the Savukoski group, the Kittilä suite, and the Kumpu group. The Salla group (2.50 – 2.44 Ga) consists of felsic to intermediate volcanic rocks and minor conglomerate breccias; the most common rocks are andesite, dacite, and rhyolite (Manninen, 1991; Hanski and Huhma, 2005). The Kuusamo group (2.44 – 2.38 Ga) consists of basaltic mafic volcanic rocks together with minor conglomerates. The Sodankylä group (2.38 – 2.22 Ga) consists of conglomerates, quartzites, siltstones, shale, carbonate rocks and mudstones (Köykkä and Luukas, 2021). The Savukoski group (2.15 – 2.05 Ga) consist of graywackes, banded iron formations (BIFs), black schists, mafic to ultramafic volcanic rocks, minor carbonates, and tuffites, as well as peridotitic komatiites (Lehtonen et al., 1998; Hanski and Huhma, 2005; Niiranen et al., 2019). The Kittilä suite (2.15 – 2.05 Ga), which consists of submarine Fe and Mg-rich tholeiitic volcanic rocks, oxide-carbonate banded formations with Fe sulfide-bearing phyllites, and affiliated sedimentary schists (Lehtonen et al., 1998; Hanski and Huhma, 2005; Wyche et al., 2015; Niiranen et al., 2019). The Kumpu group (<1.90 Ga) consists of conglomerates, quartzites, and minor felsic volcanics (Lehtonen et al., 1998; Ahtonen et al., 2007; Wyche et al., 2015). Greenschist alteration is very common within the study area, together with brecciation, veining and other alterations such as albitization (Hölttä et al., 2007; Wyche et al., 2015). Albitization dominates within the Kiistala shear zone. A mix of carbonate-quartz is found within the brecciated and veined areas. Albitization occurs commonly with the ore of Kittilä mine (Wyche et al., 2015). Sometimes albitization can be encountered in the fresh mafic rock. The lithological rock units covered by study areas 1 and 2 are illustrated in Fig. 2.

Kuotko, also known as Iso-Kuotko, is a gold deposit within the central Lapland belt. It consists of tholeiitic volcanic rocks (Härkönen et al., 2000). These rocks have been metamorphosed at greenschist facies (Härkönen et al., 2000). Gold is structurally controlled and hosted by a sulfide-bearing quartz-carbonate vein system; the majority of the gold can be found as load style free milling and the rest as refractory within arsenopyrite and pyrite (Härkönen et al., 2000).

Suurikuusikko deposit, also referred to as Kittilä mine, is the Agnico Eagle's gold mine. The deposit is hosted by tholeiitic mafic volcanic rocks. These rocks have been deformed by the Kiistala shear zone. Gold is mostly (~95 %) found as solid-solution lattice substitutions in arsenopyrites and (arsenian) pyrites (Kojonen and Johanson, 1999; Wyche et al., 2015). Native Au can be found as inclusions as well as various alloys with Ag and Hg (Chernet et al., 2000; Wyche et al., 2015). Other minerals associated with the ore are gersdorffite (NiAsS), chalcopyrite ($CuFeS_2$), chalcocite ($Cu_2S$), sphalerite ((Zn,Fe)S), pyrrhotite ($Fe_{1-x}S$), monazite ((REE,Th,Ca)$PO_4$), ullmannite (NiSbS), berthierite ($FeSb_2S_4$), gudmundite (FeSbS), bournonite ($PbCuSbS_3$), galena (PbS), jamesonite ($Pb_4FeSb_6S_{14}$), bornite ($Cu_5FeS_4$), chromite ($(Fe,Mg)Cr_2O_4$), talnahkite ($Cu_9(Fe,Ni)_8S_{16}$), and tetrahedrite ($(Cu,Fe)_{12}Sb_4S_{13}$) (Kojonen and Johanson, 1999; Chernet et al., 2000; Aho, 2009). The mineralization is associated with intense albite and carbonate(-sericite) alteration (Wyche et al., 2015).

Moreover, Fennoscandia hosts numerous mafic-ultramafic intrusions where many of them contain significant deposits of Cr, Ni–Cu, PGEs, V and Ti (Maier and Hanski, 2017). When considering Finland, PGE-Cr-V and Ni are hosted mostly within magmatic deposits. As an example, PGE deposits in the Tornio-Näränkävaara belt (Portimo, Penikat, Koillismaa), Cr deposits in the Kemi intrusion, V-hosted Koillismaa, Koitelainen and Akanvaara intrusions, Ni–Cu-PGE in the Kevitsa and Sakatti deposits (Maier et al., 2015). The Central Lapland belt in Finland is

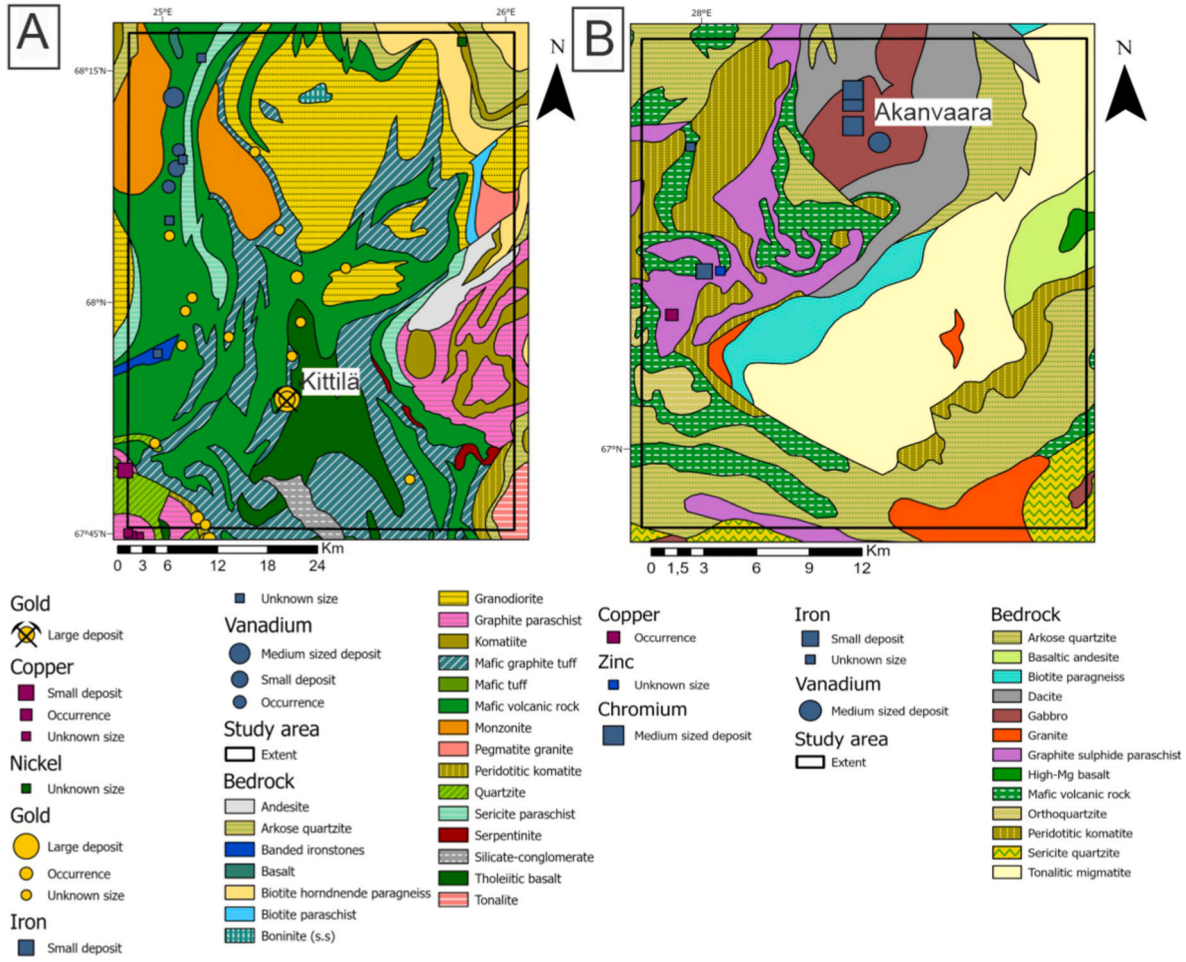


**Fig. 2.** Lithological rock units covered by A) study area 1 and B) study area 2. The lithological map is constructed using digital map information from the GTK Maankamara: http://gtkdata.gtk.fi/Maankamara/index.html © Geological Survey of Finland (2015, GTK Basic license version 1.1), Bedrock of Finland 1:100000 (2023–2024), CC-BY-4.0.

associated with four main generations of mafic-ultramafic intrusions. The first event was around ~2.44 Ga, which resulted in large, layered intrusions like Koitelainen and Akanvaara. These intrusions cut the Salla group volcanic rocks and contain reef-type Cr–V–Ti and PGE mineralization. The second event (~2.22 Ga) was associated with Haaskalehto diabase sills that intruded the Sodankylä group, whereas the third event took place around ~2.15 Ga with intrusions cutting the upper parts of the Sodankylä group and lower parts of the Savukoski group sediments (Hansen et al., 2023). During this period, differentiated mafic-ultramafic intrusions had resulted in the eastern parts of the central Lapland belt, such as Rantavaara minor contact type Cu–Ni intrusion and Co–Cu-(Au) mineralization in the Tanhua area. The fourth event (~2.05) associates with most of the ultramafic magmatism-related Cu–Ni-PGE deposits in the central Lapland belt, such as the Kevitsa and Sakatti deposits (Hanski and Huhma, 2005; Maier and Hanski, 2017).

The Akanvaara mafic layered intrusion, which is located in the study area 2 is a V–Cr-PGE deposit. It hosts 23 Cr layers and numerous Cr bands. The layers have been divided into four groups; these are upper chromite (UC), uppermost lower chromite (ULC), lower chromite (LC) and lowermost lower chromite (LLC) (Mutanen, 1997). The upper layers have discrete solitary Cr layers, while the lower layers consist of multiple groups of layers. The thickness of layers ranges from a few centimetres to 2-3 m. The host rock is amphibolite facies metamorphic grade (Mutanen, 1997). Apart from that, Kevitsa hosts a large, disseminated Ni–Cu-(PGE) sulfide deposit in the lower ultramafic part of the intrusion. Olivine pyroxenite is the host rock for sulfide ore. Moreover, three Olivine cumulate bodies (main body, northeast and southwest satellite bodies) host the Sakatti deposit. There, sulfide ores hosting Ni, Cu and PGEs occur as massive, semi-massive, disseminated and stock work veins. The massive ore can be subdivided into Ni-dominant and Cu-dominant types, while the remaining ore types are Cu-dominated. The ore mineral assemblage consists of chalcopyrite, pyrrhotite, pentlandite, pyrite, magnetite, and PGE-Ni tellurides, hosted primarily in olivine cumulates, komatiitic lavas and olivine gabbronorites (Luolavirta et al., 2018; Höytiä et al., 2024).

## 3. Materials and methods

The targeting till dataset of Finland (Gustavsson et al., 1979) was used in this study and two separate sub-datasets from the central Lapland area have been extracted for the previously mentioned analysis (Fig. 1). The mineral deposit predicted maps were generated using sparse regional till datasets of Finland and were compared with the denser targeting till data set to evaluate the methodology at different sampling densities. R (software) (R Core Team, 2022), Microsoft Excel were used for data pre-processing and data analysis, whereas data interpolation and integration were done using the commercial GIS, ArcGIS 10.8.1. Analyses were done for the isometric log ratio (ilr) converted data. Table 1 presents the sampling density of each layer identified using two separate till depth level classification methods, along with the corresponding concentration ranges of elements within each layer. Fig. 4 shows the sampling density maps for each identified depth

**Table 1**
Summary table of mean element concentrations in till, sampling density, and total number of data points by depth intervals.

| | Depth (m) | Total points | Point density (n/km$^2$) | Mean concentration (ppm) | | | | | | | | |
|---|---|---|---|---|---|---|---|---|---|---|---|---|
| | | | | Ca | Co | Cr | Cu | Fe | Mg | Ni | Ti | V |
| Gold maps | 0.0–1.0 | 5853 | 2.076 | 7583.7 | 19.5 | 177.7 | 65.3 | 60328.7 | 15521.2 | 76.5 | 7415.6 | 324.3 |
| | 1.0–2.0 | 11797 | 4.183 | 8726.9 | 23.1 | 205.6 | 88.2 | 75509.0 | 18102.1 | 96.8 | 6898.8 | 350.0 |
| | 2.0–3.0 | 3038 | 1.077 | 11093.1 | 24.3 | 226.4 | 99.8 | 78258.8 | 18786.8 | 105.6 | 6772.8 | 375.4 |
| | 3.0–4.0 | 1565 | 0.555 | 12855.3 | 25.4 | 224.5 | 104.4 | 80569.5 | 19227.6 | 107.1 | 6850.7 | 394.4 |
| | 0.4–1.0 | 5827 | 2.085 | 7789.2 | 19.5 | 177.0 | 64.4 | 60174.2 | 15679.9 | 75.3 | 7369.8 | 322.2 |
| | 1.0–1.7 | 5174 | 1.847 | 8896.2 | 22.8 | 196.8 | 82.3 | 69548.8 | 17733.4 | 90.8 | 7218.5 | 348.2 |
| | 1.7–3.6 | 9083 | 3.235 | 9144.6 | 23.6 | 214.1 | 95.2 | 79268 | 18446.5 | 102.9 | 6718.5 | 361.1 |
| | 3.6– 10 | 1808 | 0.643 | 15152.7 | 25.7 | 234.5 | 105.9 | 79389.2 | 19884.6 | 110.1 | 6920.2 | 397.9 |
| Orthomagmatic maps | 0.0–1.0 | 1617 | 2.035 | 16266.3 | 23.5 | 691.2 | 83.3 | 87486.2 | 26351.7 | 269.9 | 8819.1 | 442.9 |
| | 1.0–2.0 | 4616 | 5.806 | 18193.7 | 27.1 | 770.6 | 106.1 | 97761.6 | 31001.4 | 319.4 | 8915.2 | 488.0 |
| | 2.0–3.0 | 1220 | 1.520 | 22843.7 | 27.9 | 807.4 | 120.6 | 93480.8 | 33084.9 | 327.6 | 8770.6 | 496.3 |
| | 3.0–4.0 | 651 | 0.826 | 26018.3 | 28.6 | 779.2 | 106.8 | 96430.8 | 35194.1 | 326.9 | 8710.0 | 487.4 |
| | 0.5–1.5 | 2386 | 3.058 | 16726.9 | 25.4 | 735.9 | 96.3 | 92224.8 | 28511.3 | 303.4 | 8877.4 | 458.6 |
| | 1.5–2.8 | 3817 | 4.892 | 18599.4 | 26.9 | 780.5 | 105.1 | 97476.7 | 31052.9 | 315.2 | 8917.2 | 494.3 |
| | 2.8–5.2 | 1087 | 1.393 | 24127.8 | 27.8 | 793.4 | 105.1 | 92341.6 | 33370.9 | 311.6 | 8844.2 | 506.3 |
| | 5.2–9.5 | 232 | 0.297 | 28266.9 | 29.4 | 696.4 | 107.6 | 99995.5 | 36898.0 | 322.3 | 8517.3 | 472.9 |

interval concerning the study areas and deposit types.

### 3.1. Methodology

#### 3.1.1. Data transformation and levelling

Target till geochemistry data (Gustavsson et al., 1979) obtained by sampling techniques other than percussion drilling or test pits were rejected. From the sediment sample dataset, only the till and weathered bedrock sample data were chosen, while all other sample types were rejected. The data set consists of 17 elements, including Si, Al, Fe, Mg, Ca, Na, K, Ti, V, Cr, Mn, Co, Ni, Cu, Zn, Pb, and Ag.

Data points recorded as below the detection limit were replaced with half of the reported detection limit. The values over the upper detection limit were used as recorded. Elements for which the majority of the data points showed below detection limit concentrations (>90 %) (Zn, Pb and Ag) were not used in data analysis. Any data point marked with a question mark (?) or asterisk (*) was removed. Isometric logratio (ilr) transformation was used for the remaining elements, which were Si, Al, Fe, Mg, Ca, Na, K, Ti, V, Cr, Mn, Co, Ni, and Cu. Element concentrations given in percentages were converted to ppm before ilr transformation. After levelling using ilr values, the fixed values were transformed to centered logratio (clr) for clearer visualization.

Log ratio transformations are based on Aitchison's (1982, 1983 and 1986) compositional data analysis (CoDA) work. Log ratio transformations can be represented in their own coordinate systems; the so-called log ratio coordinates. These are linked to Aitchison geometry (Pawlowsky-Glahn and Ergozcue, 2001). Ilr-coordinates are a method of log ratio transformations in which a composition x, is expressed by a vector z or rather

$$ilr(x) = z = (z_1, \ldots, z_{D-1})' \tag{1}$$

with

$$z_j = \sqrt{\frac{D-j}{D-j+1}} \ln \frac{x_j}{\sqrt[D-j]{\prod_{k=j+1}^{D} x_k}} \quad for\ j = 1, \ldots, D-1 \tag{2}$$

(Fišerová and Hron, 2011). Where D is the dimensions given to the vector z, in other words, the number of inserted or used variables. The resulting vector z, then, is "missing" one variable in accordance with D–1 (Filzmoser et al., 2018) (eq. (1)). For example, in this study, the missing variable is copper. Even though the last variable is not taken into the results, it is still accounted for in the geometric mean.

The resulting ilr-coordinates are called pivot coordinates, where the first part or the first ilr-value is set to be a pivot (Filzmoser et al., 2018). The first compositional part or the pivot value ($x_1$) describes the relative dominance of the first variable against the geometric mean of the rest (Filzmoser et al., 2018). Subsequent values could be interpreted to represent the relative dominance of the variable minus previous variable (s).

The clr-coefficients are a transformation method where a composition x is expressed by a vector y in equation (3).

$$y = clr(x) = (y_1, \ldots, y_D)' = \left( \ln \frac{x_1}{\sqrt[D]{\prod_{k=1}^{D} x_k}}, \ldots, \ln \frac{x_D}{\sqrt[D]{\prod_{k=1}^{D} x_k}} \right) \tag{3}$$

When compared to ilr, the clr has certain advantages. First, as can be seen from the comparison of equations (2) and (3), the clr ends up with D components rather than D – 1, as in ilr. The other advantage is that clr values can be understood as coefficients instead of coordinates. In clr, all parts are dependent on each other. To elaborate this, $x_1$ is not exclusively associated with $y_1$, log ratio information of $x_1$ is accounted in $y_2$, $y_3$, …, $y_D$ (Filzmoser et al., 2018).

After transforming the data to ilr form, a levelling method was used. Several styles of levelling methods for data that have noticeable concentration differences, or level differences, have been proposed (e.g., Pereira et al., 2015; Pereira et al., 2016; Main and Champion, 2022). In a case where the data points do not overlap but are still short distances away, the aforementioned methods do not apply. An example of this is, where the sampling campaign has been conducted according to map sheets and their boundaries. In other words, the data points do not overlap, up to an accuracy factor, the coordinates might overlap. For these non-overlap situations, (Daneshfar and Cameron (1998)) proposed a method where one of the map sheets or several map sheets are deemed correct. Suppose that we have map sheets a and b, where a is the correct map sheet. Two selection zones, $s_1$ and $s_2$, are formed on both sides of the map sheet boundary, $s_1$ on the a's side and $s_2$ on the b's side. These zones are given a width, for example, 5 km. An *n* number of sample points within the zones are selected at random. For the decided elements, a q-q plot is generated. A regression line is then fitted through the plot. The function of the regression line is subsequently used as a correction function to level the element values of the map sheet b. After b's levelling, the next levelling path could be map sheets b and c. Although it should be noted that the best levelling path is the one that has the least changes in the underlying bedrock (Daneshfar and Cameron, 1998; Williams, 2021; Raatikainen et al., 2025). To achieve

the levelling as described, an R script was developed. This method was applied in ilr space, after which the fixed values were transformed back to clr values for comprehensive visualization.

### 3.1.2. Fuzzy logic

The classical set theory, where membership is designated by 0 or 1, false or true respectively, can be described as inflexible in assigning membership. In a geological context, true or false values, while helpful, cannot accurately represent the complexity of bedrock, nor surficial geology. For the processes that form these are part of a time-transgressive process, from area to area and in intensity, while still being part of the same overarching formation. If one uses true or false values for this kind of data, it could skew a lot of data points into the wrong extremes. Because of this inflexibility, the fuzzy logic was decided to be used rather than the classical set theories. Fuzzy logic is a set theory method proposed by Zadeh (1965). Where data points of a data set are given values for degrees of membership. These values are between 0 and 1, non-membership to full membership, respectively. In other words, fuzzy logic defines the degree of membership by the condition of $0 \leq x \leq 1$ (Zadeh, 1965; Bonham-Carter, 1994). Further, the value of 0.5 can be considered as random.

$$A = \{[x, \mu A(x)] | x \in X\} \tag{4}$$

where μA(x) is membership function of x in A. X is a variable, which value x is a part of. x is value.

The basis for fuzzy function is equation (4) (Zadeh, 1965). The specific function for fuzzy logic is the one that is used in the ArcGIS software. For elements that needed to have high values 'Large' was used, for elements that needed to have low values, 'Small' was used.

Spread defines the shape of the graph; in other words, it determines whether lower or higher values belong to the membership set. The spread parameter typically ranges between 1 and 10, whereas negative values may also be assigned. If a positive value is decided, then high values are set to be part of the membership group. On the other hand, if a negative value is decided, then low values are part of the membership group (Tsoukalas and Uhrig, 1997).

Midpoint defines the 0.5 membership value for the function. Usually, either mean or median is used for the midpoint value. Here, the software's defaults were used. For a graph, this means sharpening or reducing the steepness (Tsoukalas and Uhrig, 1997). After calculating fuzzy membership and forming initial fuzzy maps, element fuzzy maps, these maps can be fused together. This can be done by using three Boolean operators AND, OR and γ (Bonham-Carter, 1994).

$$\mu_{AND} = MIN(\mu_A, \mu_B, \mu_C, \ldots, \mu_n) \tag{5}$$

$$\mu_{OR} = MAX(\mu_A, \mu_B, \mu_C, \ldots, \mu_n) \tag{6}$$

where $\mu_A$, $\mu_B$, $\mu_C$, …, $\mu_n$ are combined fuzzy maps. $\mu_{AND}$ is fuzzy operator AND. $\mu_{OR}$ is fuzzy operator OR.

The operator AND (eq. (5)) is used when multiple, two or more, maps are combined, and all the evidence must have an impact on the resulting map. The OR operator (eq. (6)) is the opposite of AND, where any of the high evidence values can have an impact on the resulting map.

$$\mu_\gamma = (\mu_{AS})^\gamma \times (\mu_{AP})^{1-\gamma} \tag{7}$$

where $\mu_{AS}$ is fuzzy algebraic sum. $\mu_{AP}$ is fuzzy algebraic product. $\mu_\gamma$ is the gamma operator. γ is the gamma value in gamma operation.

Gamma operator, or γ operator, is used to combine element fuzzy maps, AND, and/or OR maps together. Gamma operator consists of two other operators, which are fuzzy algebraic sum and fuzzy algebraic product. Equation (7) ties these two functions together using a gamma value that is decided between 0 and 1, in other words $0 \leq \gamma \leq 1$ (Zimmermann and Zysno, 1980). Usually, 0 or 1 are not selected as they are too extreme. When $\gamma = 0$ the result of equation (7) behaves like an algebraic product. When $\gamma = 1$, the result corresponds to the algebraic sum. Moreover, Intermediate values of gamma control the degree of increase or decrease in the combined fuzzy membership (eq. (7)) (Bonham-Carter, 1994).

For gold deposit fuzzy maps Cu, Ni, Co, Cr, Fe, Ca, and Mg were used. The fuzzy maps were generated using ArcGIS software. For the process of fuzzification first kriging was used with the clr-values. For fuzzy overlay maps AND and OR were first used. For the AND map Cu, Ni, Fe, Cr, and Co were used. For Cu, Ni, Fe, and Co the LARGE option was used, meaning that high values would indicate membership. This is due to many of the local deposits, which are associated with gold, have a high concentration of pathfinder elements. Cu and Co, for example, are common main or secondary elements with gold deposits within the study area. Elevated Ni and Fe indicate mafic-hosted gold deposits. Whereas for Cr option SMALL was used, meaning that low values would indicate membership. This is due to Cr not being associated with gold deposits within the study area. Furthermore, based on the knowledge of mineral deposits in the area, there are no Cr deposits within the study area. These were put under the AND operator because the expectation was that all the aforementioned elements should have an impact on the result. For the OR map, Mg and Ca were used. The reasoning for these two was the prevalent hydrothermal alterations within the study area. Furthermore, many of the gold deposits in the area are structurally controlled by different hydrothermal alteration derived events (Härkönen, 1997; Kojonen and Johanson, 1999; Eilu et al., 2007; Patison, 2007; Patison et al., 2007; Hulkki and Keinänen, 2007; Saloranta, 2011). Such alterations include albitisation and/or carbonatization. These two elements were assigned under the OR operator due to the expectation that either of them can have an impact on the results. These two overlay maps were merged using the gamma operator. For the gamma operator, the value 0.8 was utilized. The 0.8 was decided so that the results are not too large, to avoid them being too close to the algebraic sum, whilst simultaneously the function would be slightly increasing (see Fig. 3).

Fuzzy overlay maps aimed at detecting orthomagmatic deposits concerning area 2 were generated using the selected elements Ni, Cu, Cr, Ti, V, Mn, Fe and Mg. The clr transformed element groups Ni–Cu–Cr, Ti–V–Mn and Fe–Mg were separated and interpolated maps were generated for each element using the kriging method. Ni, Cu and Co are commonly associated with sulfide minerals in ultramafic or mafic rocks. Thus, grouping them highlights the sulfide-rich mafic-ultamafic areas, which are the main target for orthomagmatic deposits (Rajamani and Naldrett, 1978). Ti, V and Cr are typically hosted in oxide minerals, which cause layered sequences in mafic-ultramafic intrusions (Hughes et al., 2021). Mg and Fe are the major rock-forming elements and enrichment of those elements represents mafic-ultramafic compositions, which helps to differentiate lithologies. Then the individual element maps were given the "Large" membership for fuzzy overlay, emphasizing the areas with higher concentrations of selected elements. Following that, the interpolated element maps of previously mentioned groups were overlaid using the OR operator separately. Ultimately, the resultant maps were integrated using the Gamma operator, where the value was 0.9, which delivered the most effective results after testing several values (see Fig. 3).

### 3.1.3. Interval approach to till stratigraphy

In the areas having multiple glacial advance phases and complex stratigraphy, different till beds/units should be considered in planning the till sampling campaign and when analysing geochemical laboratory results. Different till units typically represent variable source areas, transport directions and distances, which can be seen in mineralogical and element composition of till material. Analyses of till stratigraphy can be done by a classical way based on sedimentological techniques, but in the case of thick till cover and large percussion drilling-based data coverage, comprehensive till stratigraphy is not possible to be created. In that case, the data itself can be used to analyse till bed composition

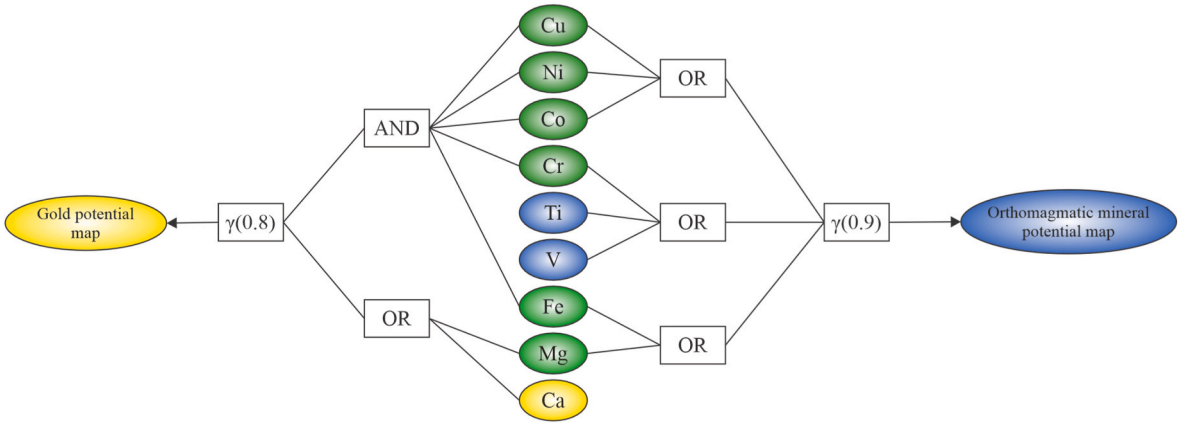


**Fig. 3.** Fuzzy flow chart for Au maps and orthomagmatic maps. Green elements are used for both sets of maps, blue only for orthomagmatics and yellow only for Au maps. (For interpretation of the references to colour in this figure legend, the reader is referred to the Web version of this article.)

and estimate the number of significant layers.

One of the tested approaches was a 1-m interval approach. In this approach, the data set was divided into 1-m intervals. Division started from the topmost till layer and continued until 4 m. The 1 m can then be taken to mean 1st meter. It includes measuring points from the ground surface to 1 m. The 2nd meter then has points deeper than 1 m to 2 m, and so on until 4 m depth. The 4-m breakpoint was decided based on the severe decrease in the number of data points. Furthermore, the average depth reported for the study area is around 2 m (Hirvas, 1991). This is supported by the mean depth of the dataset, which is approximately 2.08 m.

Within each interval of a drilled data point, multiple measuring points were recorded. The concentration values of the measuring point, within a given interval, were calculated and the average was then used. These calculations were done using the ilr-values. This was done for each interval and variable separately. The ilr-values were transformed back into clr-values for better visualization and, relative, ease of interpretation.

The other approach was studying the depth profile of the targeting till dataset by identifying depth intervals where a significant change of mean and/or variance exists. Elements Si, Fe and Mg were used to identify the depth breaks. For this purpose, the cpt.meanvar function from the library changepoint in R (R Core Team, 2022) and the pruned exact linear time (PELT) algorithm were used as the search method for multiple changepoints. From this, the points where the changes in mean and/or variance exist in the spatial dataset were identified. Then, k-means clustering was carried out to cluster the breakpoints.

The changepoint package in R can be used to identify distinct multiple shifts or changes within a single sequence. Different changepoint detect algorithms, such as the binary segmentation algorithm, segment neighbourhood algorithm, PELT algorithm are available in the package. Changepoints represent the points at which there is a change in the statistical properties of a sequence of observations, for example, variance.

In order to understand the overall method, first single changepoint detection method is explained. This involves identifying the point where a single change occurs in the dataset (changepoint). $H_0$ represents the null hypothesis which indicates that there is no changepoint and $H_1$ alternative hypothesis, which indicates there is one changepoint. Then the likelihood test is used to calculate the maximum likelihood for each case to check these null and alternative hypotheses (how well each model fits the data). It is assumed that we have an ordered sequence of data $y_{1:n} = (y_1, \ldots, y_n)$. For the null hypothesis, Maximum log likelihood is, $\log p(y_{1:n}|\widehat{\theta})$

Where p(.) is the probability density function and $\widehat{\theta}$ is the maximum likelihood estimate of the parameters. For the alternative hypothesis, a model with a changepoint at $\tau_1$, where $\tau_1 \in \{1, 2, \ldots, n-1\}$, the maximum log likelihood is given $\tau_1$ is represented by,

$$\mathrm{ML}(\tau_1) = \log p\left(y_{1:\tau_1}|\widehat{\theta_1}\right) + \log p\left(y_{(\tau_1+1):n}|\widehat{\theta_2}\right)$$

Test statistics denoted by $\lambda$ is used to test the hypotheses, $\lambda = 2\left[\max_{\tau_1} ML(\tau_1) - \log p(y_{1:n}|\widehat{\theta})\right]$

Where the maximum log likelihood value of the alternative is $\max_{\tau_1} ML(\tau_1)$. A threshold c is used to determine whether to reject the null hypothesis. If the test statistics $\lambda$ >c, it suggests that the data likely accommodate a changepoint at $\tau_1$. Furthermore, this method can be expanded to find multiple changepoints as well, by summing up the likelihood for each of the m segments. Following is the function for the multiple changepoint detection, and the most common approach is to minimize (8),

$$\sum_{i=1}^{m+1}\left[C\left(y_{(\tau_{i-1}+1):\tau_i}\right)\right] + \beta f(m) \quad (8)$$

where C is a cost function for a segment, as an example; negative log-likelihood and $\beta f(m)$ is the penalty term to control the number of changepoints and avoid overfitting. When detecting multiple changepoints, it is essential to effectively estimate the location of different changepoints. The main search methods available to detect changepoints within the changepoint package are binary segmentation, segment neighbourhoods and PELT. In binary segmentation, first a single changepoint test statistic is applied to the whole data, and the data is split into two, if a changepoint is identified. Then the single changepoint procedure is performed on the two new datasets. After that, the datasets will be split further, if changepoints were identified, and this continues until no more changepoints are identified. This is a very fast and approximate method. The segment neighbourhood algorithm finds the optimal solution for m+1 changepoints using results from m. This algorithm is exact and is computationally complex and slower than binary segmentation. The PELT algorithm combines the best of both binary segmentation and segment neighbourhood, where the algorithm is similar to the segment neighbourhood algorithm that results in exact segmentation. This is computationally efficient as it uses mild assumptions (Killick and Eckley, 2014).

Fig. 4 illustrates the depth intervals that have been used by two distinct methods, fixed interval and statistics-based, together with the distribution of sampling points within those depth intervals across selected study areas.

### 3.1.4. Map model validation

A receiver operating characteristic curve (ROC) (Obuchowski, 2003)

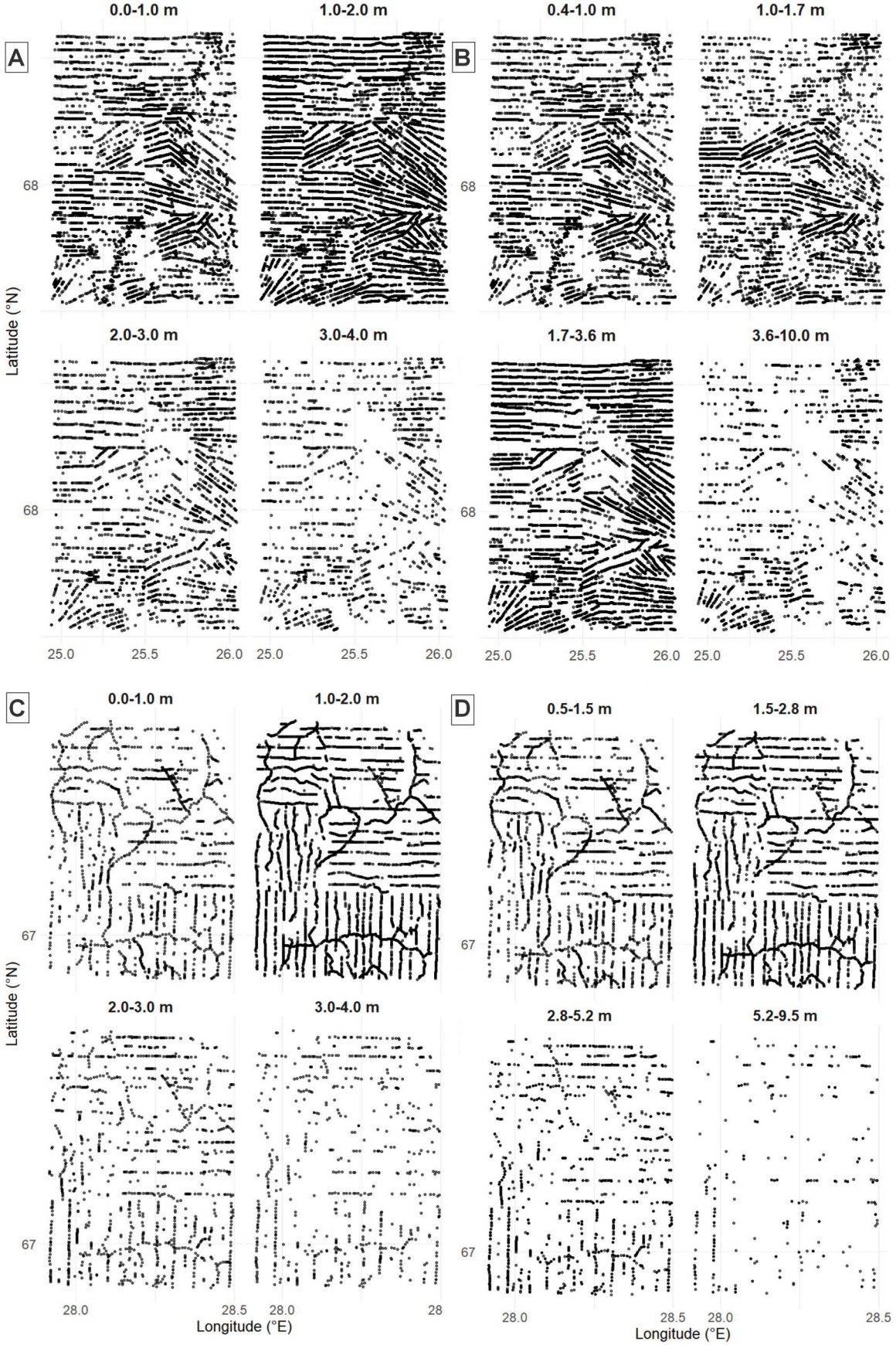


**Fig. 4.** Sampling point density maps for A) gold area concerning fixed depth intervals B) gold area concerning statistical-based depth intervals C) Orthomagmatic area concerning fixed depth intervals D) Orthomagmatic area concerning statistical-based depth intervals.

was used for validating the results. ROC is a classifier used to illustrate the performance of a model. In the ROC approach, the true positive rate (TPR) is plotted against the false positive rate (FPR). Or in other words, sensitivity (probability of detection) is plotted against 1 – sensitivity (probability of false alarm).

In geology, the TPR can be considered to mean known mineral occurrences and/or deposits. To get the FPR, one needs the true negative rate (TNR). TNR can be considered to mean no known mineral occurrences and/or deposits. Nykänen et al. (2015) suggest that for the purposes of TNR, either other deposit types or randomly selected points may be used. In this study, random points were used due to the small number of different deposit types within the study area.

To validate which ROC graph is "better", the area under the curve (AUC) can be utilized. The AUC method calculates the area between the ROC curve and x-axis; in other words, the area under the ROC curve. The best model is the graph that has the highest AUC value. Based on the descriptions of ROC and AUC above, in this study, the result of ROC and AUC can be interpreted as better than, or worse than, random points (see for Nykänen et al., 2015; Sarala and Nykänen, 2017). However, ROC curves do not take into account the occupied areas of predicted targets, even though it is a crucial factor when assessing the performance of different mineral prospectivity models (Roshanravan et al., 2019). In addition, points representing negative deposits and/or occurrences were generated randomly while keeping a 2 km buffer around known deposits. Thus, this may have a negative effect on the validation results obtained using the ROC method in this study.

#### 3.1.5. Prediction–Area plot (P–A plot)

The Prediction–area (P–A) plot was also used to validate the fuzzy overlay maps. These models can be used to evaluate how well the predicted overlay maps capture known mineral deposits within a smallest possible targeted area. According to Roshanravan et al. (2019), the locations of known mineralisations can be used to validate the prospectivity models in mineral prospectivity mapping and the reliability of maps depend on the strength of geological signal and the area that signal covers. P–A plot developed by Yousefi and Carranza (2015a), uses the proportion of known mineralisations predicted by prospectivity classes and the areas covered by each prospectivity class with respect to the total area of the study. This approach was used to evaluate the different predicted maps obtained for various depth intervals in order to validate the prospectivity modes.

## 4. Results

Table 1 shows the total number of data points that lie in different till depth intervals, their density and mean values for element concentration concerning elements used in fuzzy overlay maps. Even though it is not advisable to apply classical statistical tests to compositional data (Reimann et al., 2012), the mean element concentrations for the study areas are presented in Table 1, just to provide a general overview of concentration distribution within the selected till layers. The more detailed table containing the ranges of element concentrations is included in Appendix 1.

### 4.1. Identifying depth intervals using a statistical approach

The statistical method used to detect till depth intervals is explained in the previous section. Initially, a total of 155 break points, indicating a significant change in mean and/or variance, were identified concerning study area 1. When detecting the changepoints, a composite metric of Si, Fe and Mg was used. Fig. 5A shows the initial break points (red) with respect to the full dataset (blue). Then these identified 155 change points were clustered using k-means clustering. According to the elbow method, the optimal number of clusters was 4 and eventually, the method delineated four depth intervals: 0.4–1.0 m, 1.0–1.7 m, 1.7–3.6 m and 3.6–10.0 m concerning study area 1. Furthermore, when considering the area focused on orthomagmatic deposits (study area 2), initially 65 breakpoints (Fig. 5B) were identified using the same statistical method and the optimal number of clusters for this area was four as well. Thus, after applying k-means clustering, four main depth intervals were identified: 0.5–1.5 m, 1.5–2.8 m, 2.8–5.2 m, and 5.2–9.5 m.

### 4.2. Interval maps

#### 4.2.1. Maps for the Kittilä area

Fig. 6 shows the fuzzy overlay maps generated using the fixed interval approach. Fuzzy logic was used to create the prospective maps for each interval. For fuzzy logic, Cu, Ni, Co, Cr, Fe, Ca, and Mg were used. Cu, Ni, Co, Cr, and Fe were used for the AND map. Ca and Mg were used for the OR map. The AND and OR maps were combined using the gamma operator with a value of 0.8 (Fig. 3). The resulting four prospection maps that define the most favourable for possible new gold deposits (Fig. 6). To generate these maps ArcGIS software's 'Fuzzy Membership' and 'Fuzzy Overlay' tools were used.

Fig. 7 illustrates the fuzzy overlay maps concerning the statistical approach for till profile in study area 1. The same fuzzy overlay formula that was mentioned in the former paragraph for fixed depth intervals was used to generate the maps for statistically defined depth intervals. The fuzzy overlay maps concerning depth intervals from the statistical method (7A, B) are almost visually similar to those generated using the

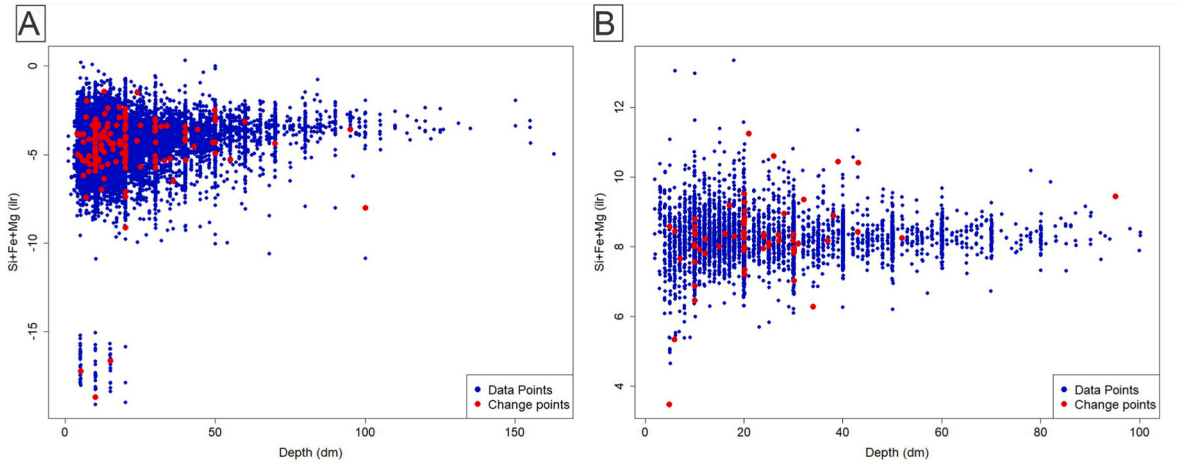


**Fig. 5.** (A) Original data points and changepoints concerning the study area 1 (Kittilä area) (B) original data points and changepoints concerning the study area 2 (Akanvaara area).

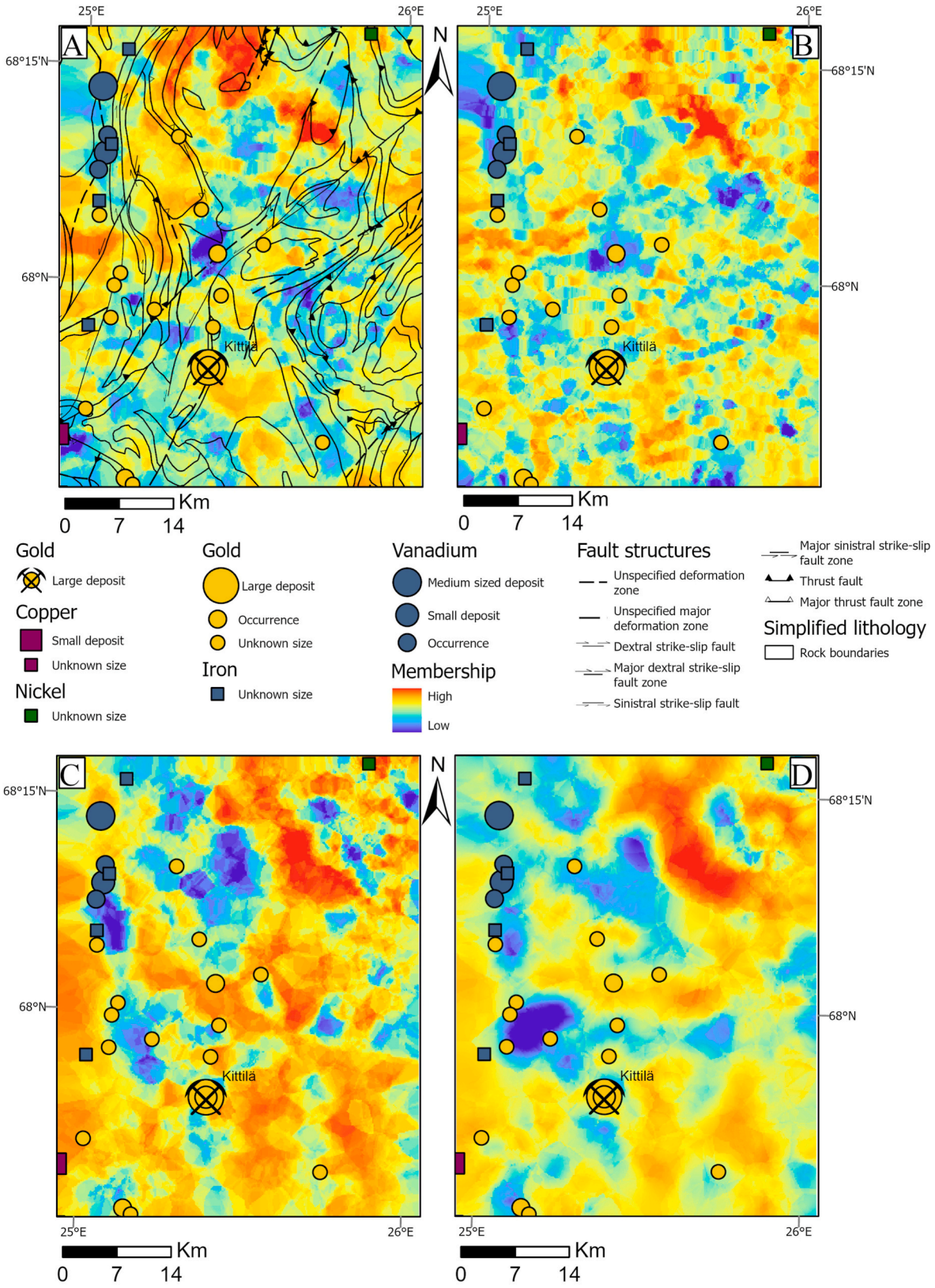


**Fig. 6.** Meter interval fuzzy prospection maps. (A) Illustrates the memberships for 0 – 1 m, (B) illustrates memberships for 1 – 2 m, (C) shows membership for 2 – 3 m, and (D) shows membership for 3 – 4 m. Lithological boundaries are shown in map 6A. The lithological map is constructed using digital map information from the GTK Maankamara: http://gtkdata.gtk.fi/Maankamara/index.html © Geological Survey of Finland (2015, GTK Basic license version 1.1), Bedrock of Finland 1:100000 (2023–2024), CC-BY-4.0.

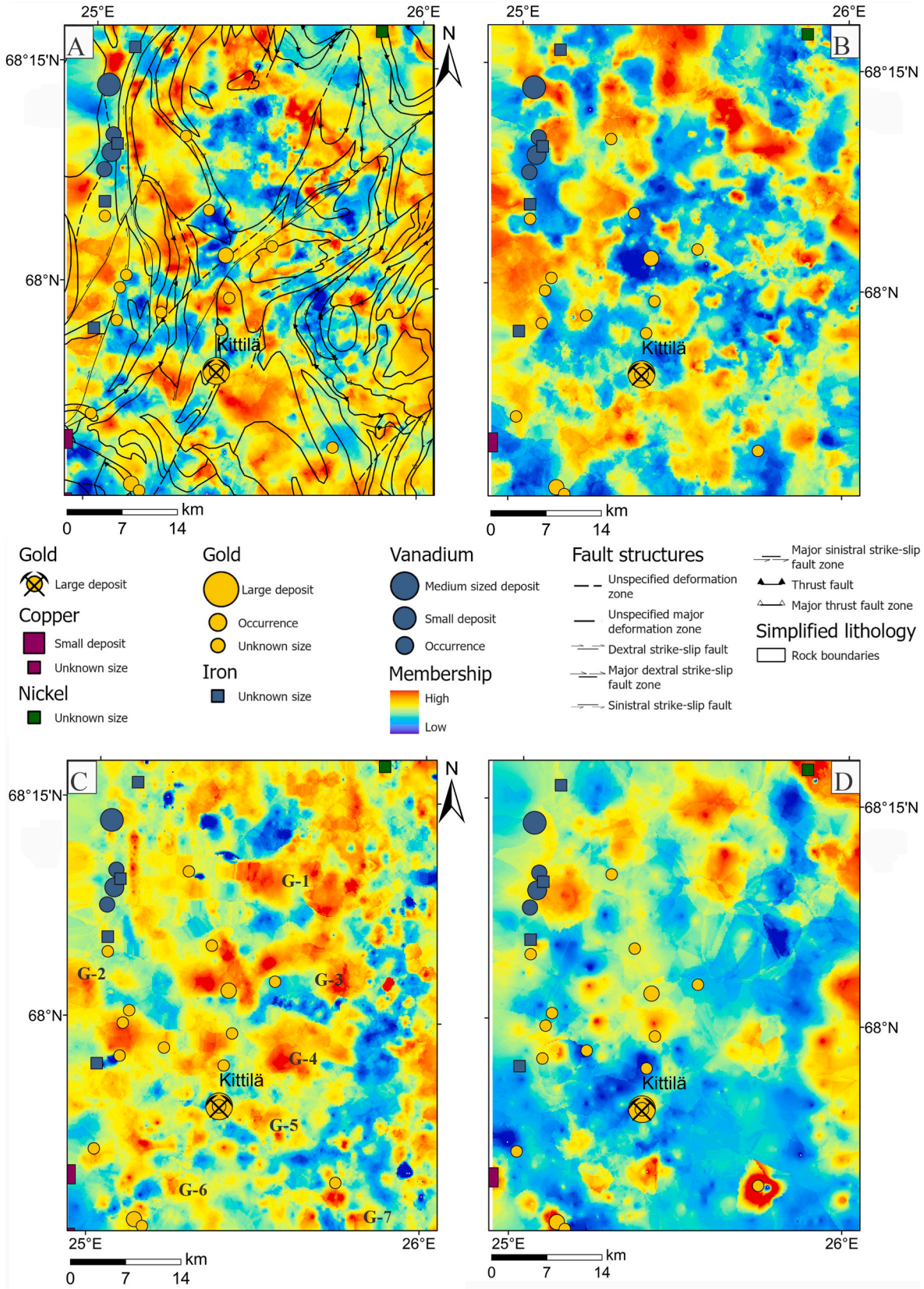


**Fig. 7.** Fuzzy prospection maps. (A) Illustrates the memberships for 0.4 – 1.0 m, (B) illustrates memberships for 1.0 – 1.7 m, (C) shows membership for 1.7 – 3.6 m, and (D) shows membership for 3.6 – 10.0 m. In addition to Kittilä mine and known Au deposits, other prominent Au anomalies have been marked as G-1 to G-7 in Fig. 7C. Lithological boundaries are shown in map 7A. The lithological map is constructed using digital map information from the GTK Maankamara: http://gtkdata.gtk.fi/Maankamara/index.html © Geological Survey of Finland (2015, GTK Basic license version 1.1), Bedrock of Finland 1:100000 (2023–2024), CC-BY-4.0.

fixed interval method (Fig. 6A and B). However, differences are clear evident in maps C and D between the two methods. Both methods indicate anomalies at the well-known Kittilä mine. Furthermore, the depth interval 1.7 – 3.6 m highlights anomalies for other known deposits more clearly than the other depth intervals.

#### 4.2.2. Maps for the Akanvaara area

Fig. 8 illustrates fuzzy overlaid maps concerning fixed 1 m depth intervals of the till profile. Maps A, B and D, which are related to the depth intervals 0-1 m, 1-2 m and 3-4 m, indicate anomalies for the known orthomagmatic deposit, Akanvaara, whereas maps A, C and D show elevated values for another Ni–Cu occurrence.

Fig. 9 shows maps generated using the fuzzy overlay method concerning four depth intervals identified using significant changes in mean and variance of element concentrations (Statistical approach). All maps indicate an anomaly over the known Akanvaara deposit. The maps related to shallower till depth intervals, 0.5-1.5 m (Figs. 9A) and 1.5-2.8 m (Fig. 9B), are very similar. However, Fig. 9C and D illustrate comparably strong anomalies over other known Ni–Cu and iron deposits, which are only faintly visible in Fig. 8A and B. In contrast, Figs. 8D and 9D show a much larger anomalous area compared with other maps.

### 4.3. Regional till fuzzy overlay maps

Fig. 10 illustrates the fuzzy overlay maps for the regional till data set concerning study area 1, the area focused on finding gold deposits and study area 2, which aimed to detect orthomagmatic deposits. According to Fig. 10A, a strong anomaly could be observed over the Kittilä mine and its surrounding area, while the upper part of the map indicates less favourable for detecting gold deposits. However, Fig. 10B highlights a huge area of the map sheet as anomalous, including the known mineralizations.

### 4.4. ROC curves for the study areas

To validate and check how well fuzzyfication succeeded, ROC and AUC were used. For True positives (TP), the known deposits with gold as main, secondary or minor commodity were used. For true negatives (TN) random points were used with a caveat that the random points cannot be closer than 2 km to the TP deposits. For the first meter, AUC gave a value of 0.519 (Fig. 11A), which is slightly better than random. For the second meter AUC value was 0.611 whereas for third meter AUC value was 0.616 (Fig. 11A). Finally, the fourth meter the value was 0.824 (Fig. 11A). The AUC calculations for the intervals of the statistical method were 0.550 for the 0.4 – 1 m range (Fig. 11B). For the second and third intervals, values 0.522 and 0.632 were obtained respectively (Fig. 11B). The deepest depth interval, from 3.6 to 10 m, recorded an AUC value of 0.721 (Fig. 11B).

For the Akanvaara area, results between intervals were calculated. For the meter interval curves (Fig. 12A), the AUC value of 0.683 was obtained for the 1 m interval, followed by the values 0.641, 0.632 and 0.760 for 2-, 3-, and 4-m intervals. AUC values obtained for the statistically gained intervals (Fig. 12B) were recorded as 0.722 for 0.5 – 1.5 m, 0.656 for the till depth interval 1.5 – 2.8 m, 0.692 for 2.8 – 5.2 m depth interval and 0.64 for the deepest till depth interval representing 5.2 - 9.5 m.

### 4.5. P-A curves

#### 4.5.1. Study area 1, focused on gold deposits

P–A plots illustrate the cumulative percentage of the study area against the cumulative percentage of the known mineral deposits concerning study area 1, representing both the fixed depth interval approach (Fig. 13) and the statistical approach (Fig. 14). This contains two curves that one represents the prediction rate of known mineral deposits or occurrences captured, and the other represents the percentage of occupied study areas by each fuzzy overlay map (Yousefi and Carranza, 2015a). Yousefi and Carranza (2015b) mention that the intersection point is the point where the prediction rate equals the occupied area and it can be used as a standard to evaluate prospectivity models. They also state that a higher intersection point in P–A plot is favourable and, that means a larger number of known deposits are captured by a smaller part of the study area. According to Figs. 13 and 14, the best three depth intervals that captured more deposits within smaller areas are, 3.6-10 m and 1.7-3.6 m intervals, both capturing 62 % of deposits within 38 % of the area and the 3-4 m interval, which captured 58 % of deposit by 42 % of the study area (Table 02).

#### 4.5.2. Study area 2, focused on othomagmatic deposits

For the area focused on orthomagmatic deposits, Figs. 15 and 16 illustrate the P–A plots concerning fixed and statistically based depth interval methods respectively. The best depth intervals that captured more deposits within smaller area are, 3-4 m interval, capturing 70 % of deposits within 30 % study area, followed by 2.8-5.2 m interval, capturing 68 % of deposits by 32 % of study area and depth intervals 0–1, 1–2, 0.5–1.5, 1.5–2.8 m, captured 60 % of deposits by 40 % of study area (Table 03).

## 5. Discussion

### 5.1. Division of depth levels

#### 5.1.1. Till bed detection

A method was developed to identify the distinct till beds by detecting significant changes in the mean and/or variance of element concentrations in the till geochemical data. The method aimed to differentiate between distinct till beds, observed based on tractor excavated test pits (with a typical 5–6 m maximum depth range) reported by Hirvas (1991) in the study areas, through identifying changes in element concentrations in the targeting till geochemical data. This method was independently applied to two separate study areas.

In the Kittilä area, located in the northern part of the ice divide zone, the first identified geochemical transition occurred between the depth interval 0.4–1 m, while in the Akanvaara area, it was observed in the 0.5–1.5 m depth interval. These depth intervals correspond well with the thickness of till bed I (in the northern Finland's stratigraphy), of which the average thickness is approximately 1.3 m (Hirvas, 1991).

The second significant till layer was identified between the depths of 1–1.7 m in the Kittilä region. The reported mean thickness of till bed II of that region is around 2.5 m (Hirvas, 1991). The Akanvaara, which is located south of the ice divide zone, showed significant changes in geochemical properties between the depth interval 1.5–2.8 m. The reported mean thickness of till bed II in that region is approximately 2.6 m (Hirvas, 1991). However, in both Kittilä and Akanvaara areas, the thicknesses of geochemically defined till layers corresponding to till bed II, as identified by the statistical method, are approximately 1 m.

The third geochemical transition layers were identified between 1.7 and 3.6 m in the Kittilä area and 2.8–5.2 m in the Akanvaara area, with corresponding layer thicknesses of 1.9 and 2.4, respectively. Although the thickness of till bed III is not well-determined, the previously studied pits report a wide range from 0.5 to 6 m, within which the recognized till depth intervals fall in the depth-limited excavated test pits. Eventually, the deepest till layers in the percussion till geochemistry were identified between 3.6–10 m and 5.2–9.5 m in Kittilä and Akanvaara, respectively. These tills may correspond to the older till beds mentioned in the previous study (Hirvas, 1991).

#### 5.1.2. Fuzzy maps and ROC for finding the most favourable till depth interval for mineral exploration

The two different areas have different favourable ranges of till depths, as example, 1.7 –3.6 m for the Kittilä area and 2.8–5.2 for the

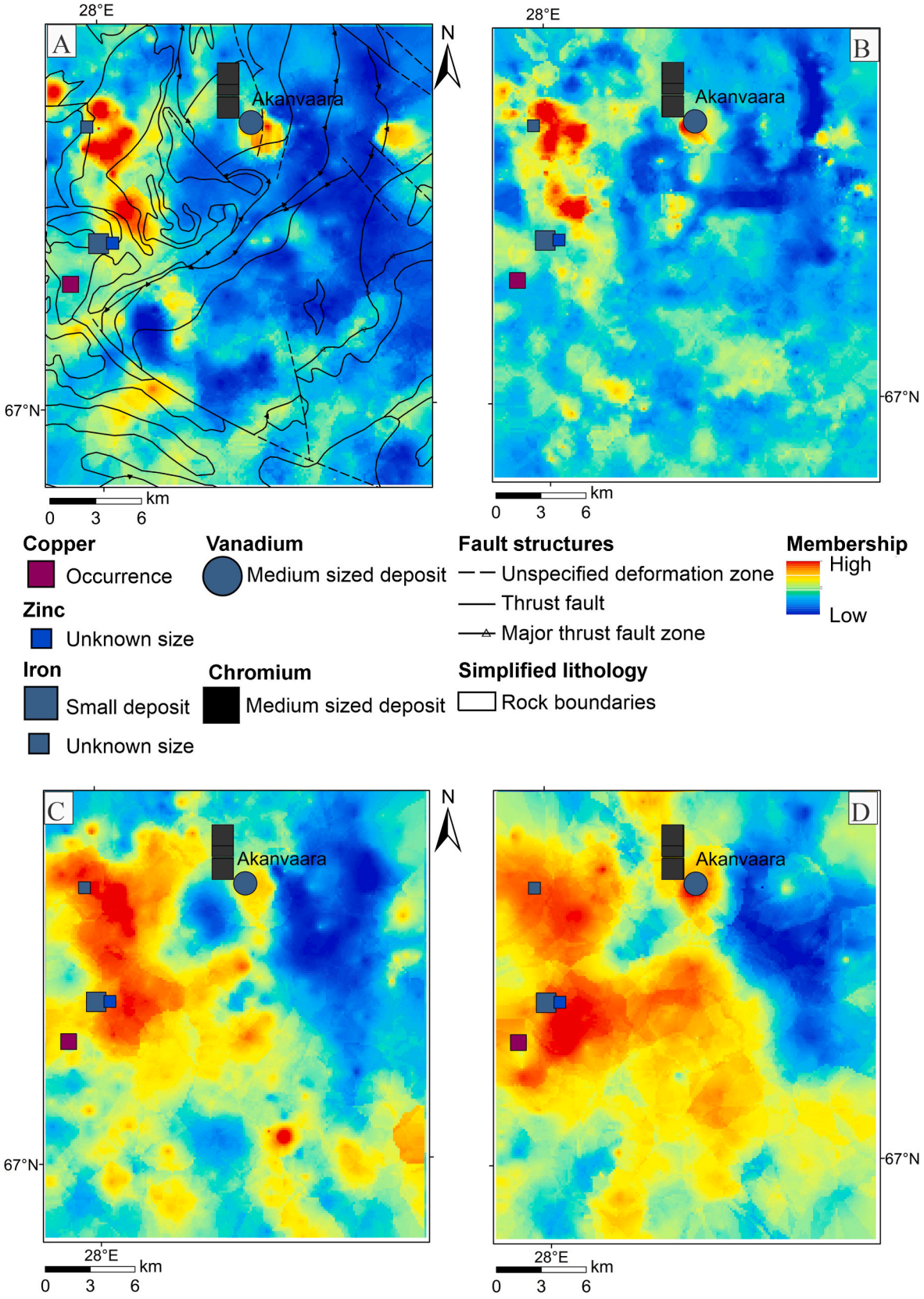


**Fig. 8.** Meter interval fuzzy prospection maps. (A) Illustrates the memberships for 0 – 1 m, (B) illustrates memberships for 1 – 2 m, (C) shows membership for 2 – 3 m, and (D) shows membership for 3 – 4.0 m. Lithological boundaries are shown in map 8A. The lithological map is constructed using digital map information from the GTK Maankamara: http://gtkdata.gtk.fi/Maankamara/index.html © Geological Survey of Finland (2015, GTK Basic license version 1.1), Bedrock of Finland 1:100000 (2023–2024), CC-BY-4.0.

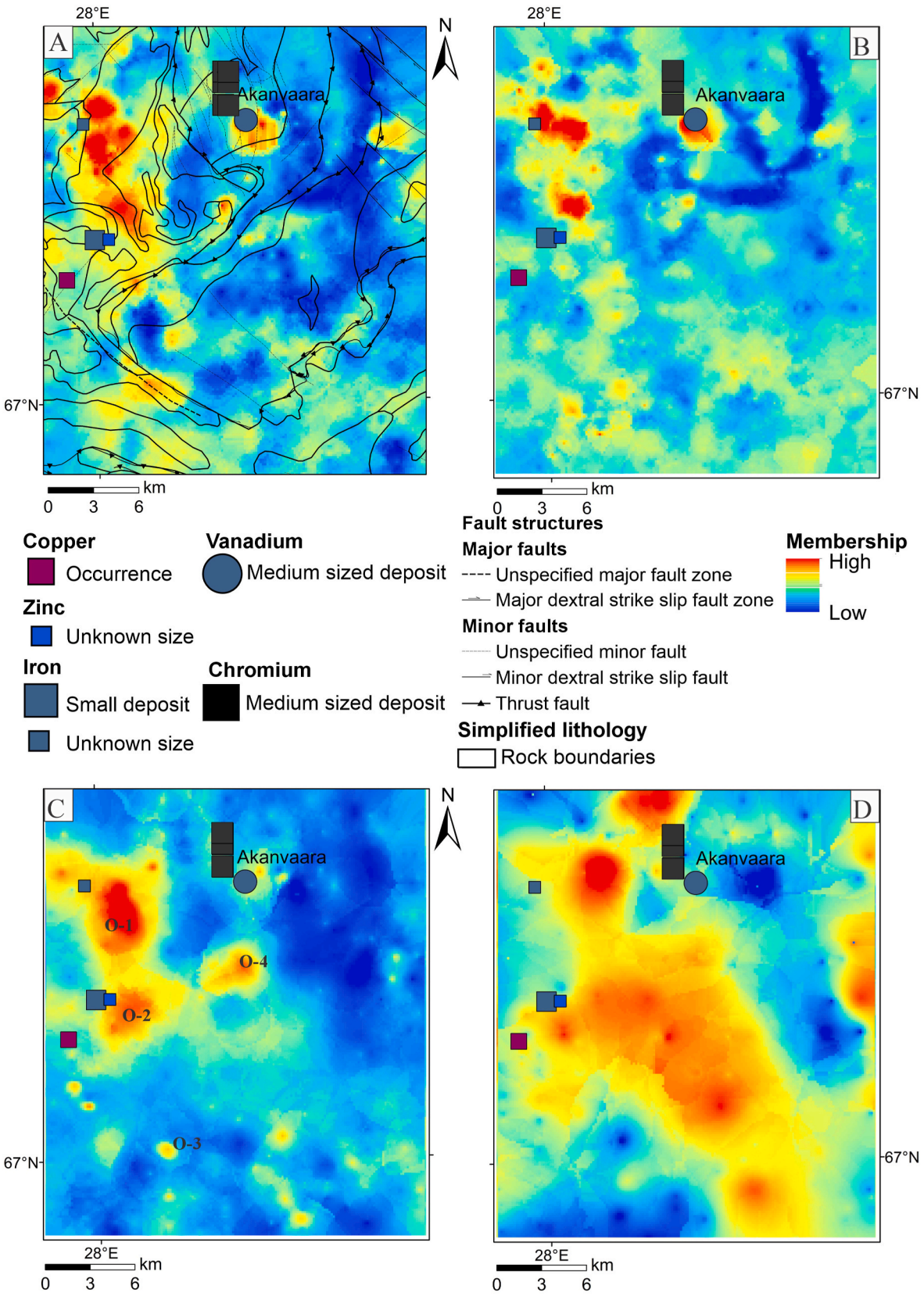


**Fig. 9.** Fuzzy prospection maps. (A) Illustrates the memberships for 0.5 – 1.5 m, (B) illustrates memberships for 1.5 – 2.8 m, (C) shows membership for 2.8 – 5.2 m, and (D) shows membership for 5.2 – 9.5 m. In addition to the Akanvaara deposit, other prominent metal anomalies related to orthomagmatic rocks have been marked as O-1 to O-4. The lithological map is constructed using digital map information from the GTK Maankamara: http://gtkdata.gtk.fi/Maankamara/index.html © Geological Survey of Finland (2015, GTK Basic license version 1.1), Bedrock of Finland 1:100000 (2023–2024), CC-BY-4.0.

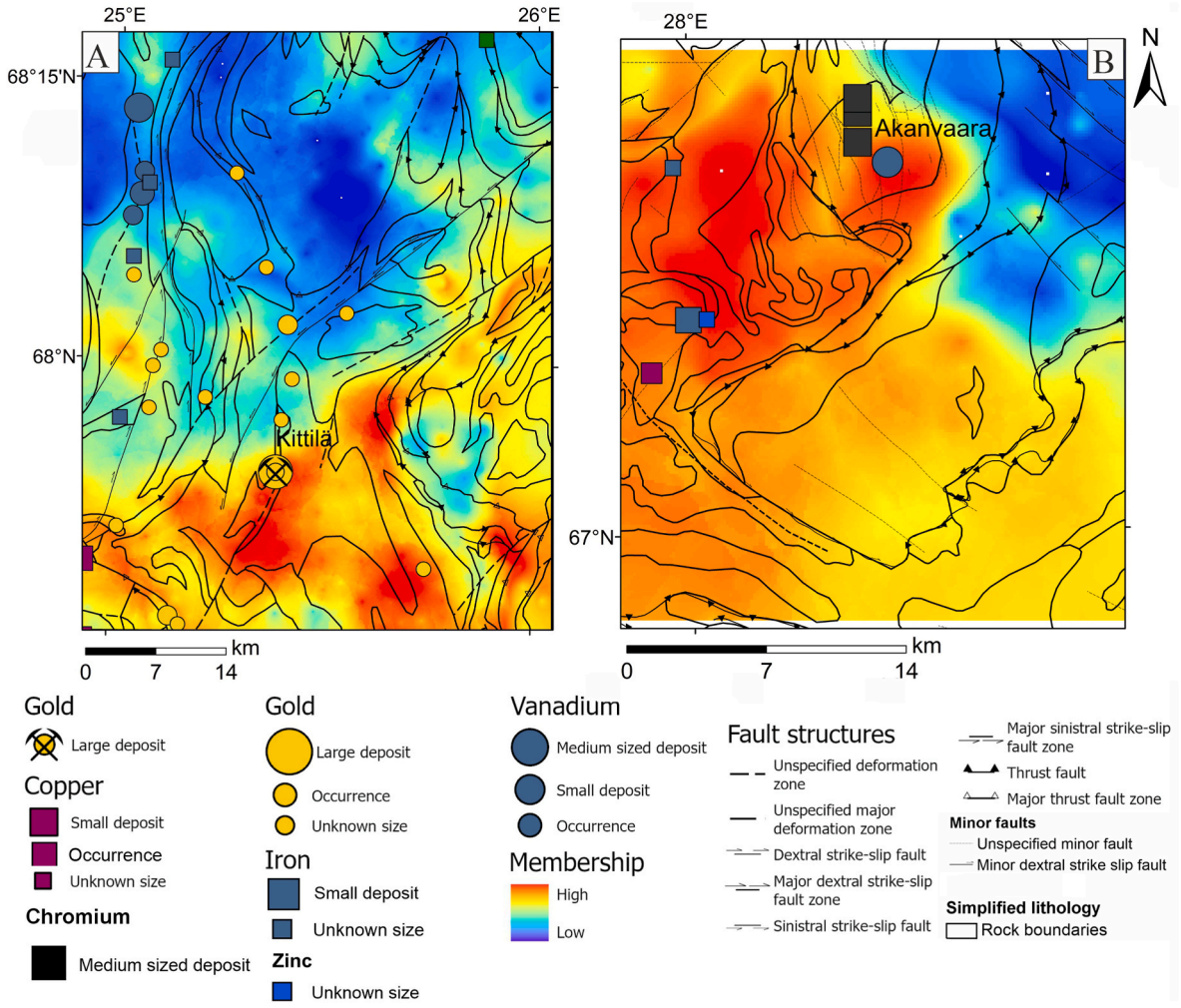


**Fig. 10.** Fuzzy prospection maps illustrate the memberships in the regional till geochemical dataset concerning (A) study area 1 - gold area, (B) study area 2 - orthomagmatic area for an average depth range of 1.5 - 2 m. The lithological map is constructed using digital map information from the GTK Maankamara: http://gtkdata.gtk.fi/Maankamara/index.html © Geological Survey of Finland (2015, GTK Basic license version 1.1), Bedrock of Finland 1:100000 (2023–2024), CC-BY-4.0. (For interpretation of the references to colour in this figure legend, the reader is referred to the Web version of this article.)

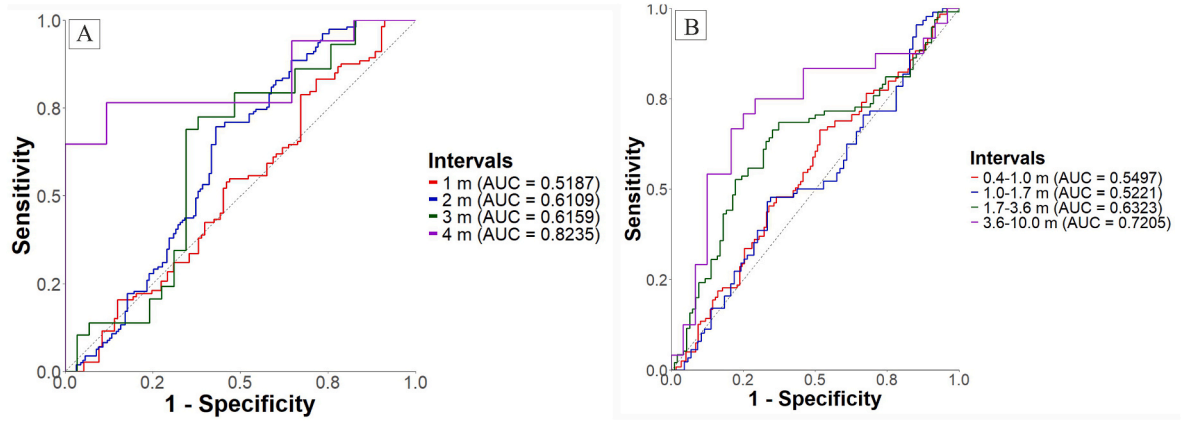


**Fig. 11.** ROC and AUC validation for Au fuzzy maps for (A) meter interval (B) intervals using statistical methods. The dashed line going from (0, 0) to (1, 1) shows the AUC value of 0.5, which can be considered totally random.

Akanvaara area to detect interested mineral deposit types. The focus was on gold deposits in Kittilä and on orthomagmatic deposits in Akanvaara. Predicted maps for the Kittilä area (Figs. 6 and 7), indicate some possible areas for new gold deposits apart from the anomalies representing known gold deposits. All fuzzy maps (Figs. 6 and 7) show an anomaly for the well-known gold deposit, Kittilä. However, the highest AUC values were obtained for 3–4 m and 3.6–10 m depth intervals, representing the fixed interval method and statistical approach method, respectively

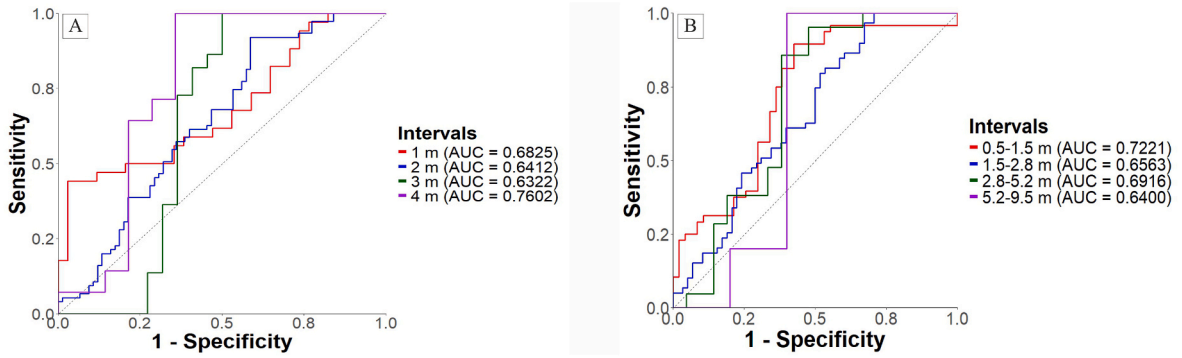


**Fig. 12.** ROC and AUC validation for orthomagmatic fuzzy maps for (A) meter interval (B) intervals using the statistical method. The dashed line going from (0, 0) to (1, 1) shows the AUC value of 0.5, which can be considered totally random.

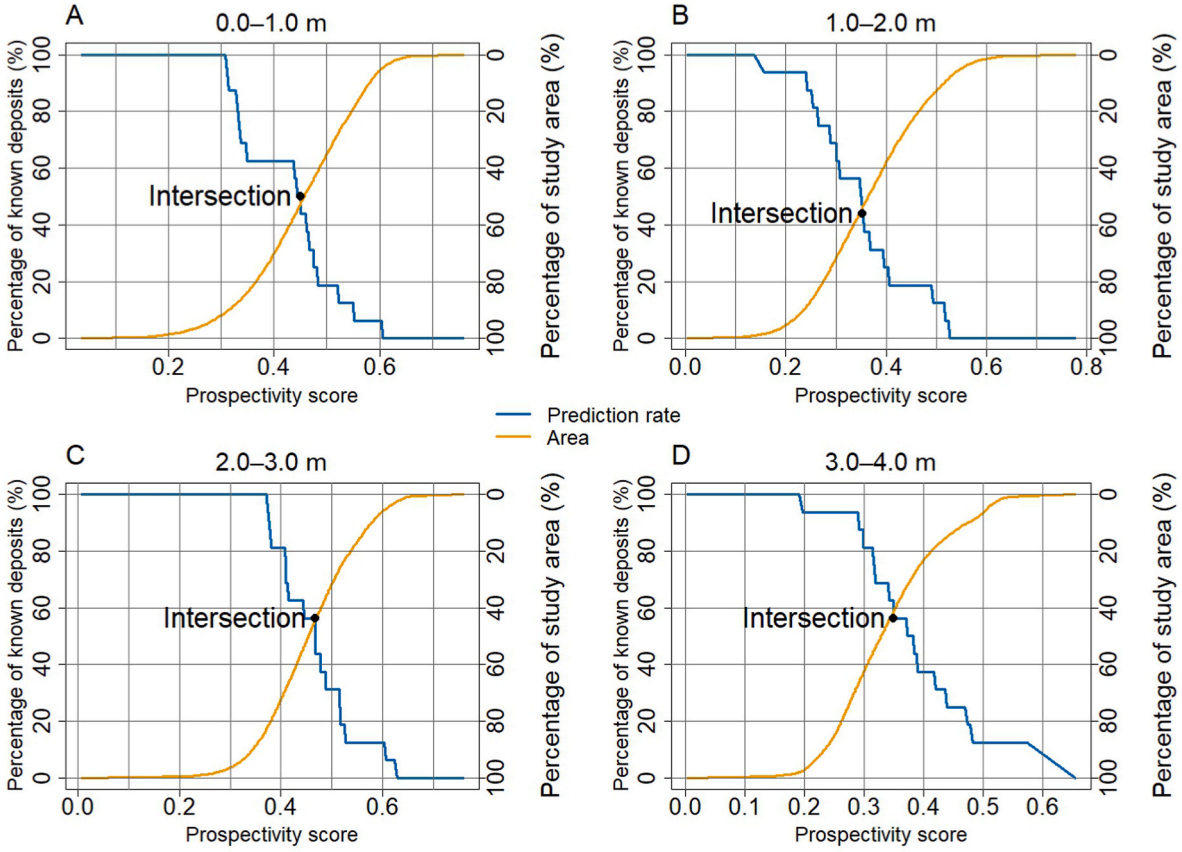


**Fig. 13.** P-A plots for different till depth intervals in study area 1 based on the fixed depth interval method.

(Fig. 11). In this dataset, although the deepest intervals had the largest AUC values, it should be noted that the number of data points decreases with depth. This decrease means that 3–4 m and 3.6–10 m depth intervals have the lowest number of data points to generate ROC curves, when compared with the other depth intervals. Thus, this factor may have affected the accuracy of the AUC value. Therefore, it was found that the highest AUC value was recorded for the till depth between 1.7 and 3.6 m (Fig. 11). Due to this, the most consistent map was obtained for the 1.7–3.6 m till depth interval (Fig. 7C). The 1.7–3.6 m interval's (Fig. 7C) counterpart would be the 3rd interval (Fig. 6C), with very similar results. However, AUC shows that the statistical method provided a slightly better result (Fig. 11). Furthermore, P–A plots support the results of the ROC analysis for the study area 1. According to Table 02, the highest percentage of known mineral deposits (62 %) is captured within the smallest percentage of the study area (38 %) for the 1.7–3.6 depth interval, after excluding the deepest depth interval, 3.6–10 m.

When considering the Akanvaara area, the fuzzy overlaid maps related to both methods are significantly similar. A strong anomaly for the Akanvaara deposit could be observed in 0–1 m, 1–2 m and 3–4 m depth intervals corresponding to the fixed interval method (Figs. 8) and 0.5–1.5 m, 1.5–2.8 m, 2.8–5.2 m, 5.2–10 m, depth intervals by the method concerning the statistical approach (Fig. 9). Although the highest AUC value was recorded in the 3–4 m depth interval, it is not totally aligned with the known lithology of area 2, as the predicted map shows a strong anomaly in the southeastern part of the map where migmatic paragneiss is present (GTK, 2024). As explained in the previous paragraph for the Kittilä area, this value may not be accurate due to the lower sampling point density. The second highest AUC value 0.7221, is associated with 0.5–1.5 m depth interval (Fig. 12), where the

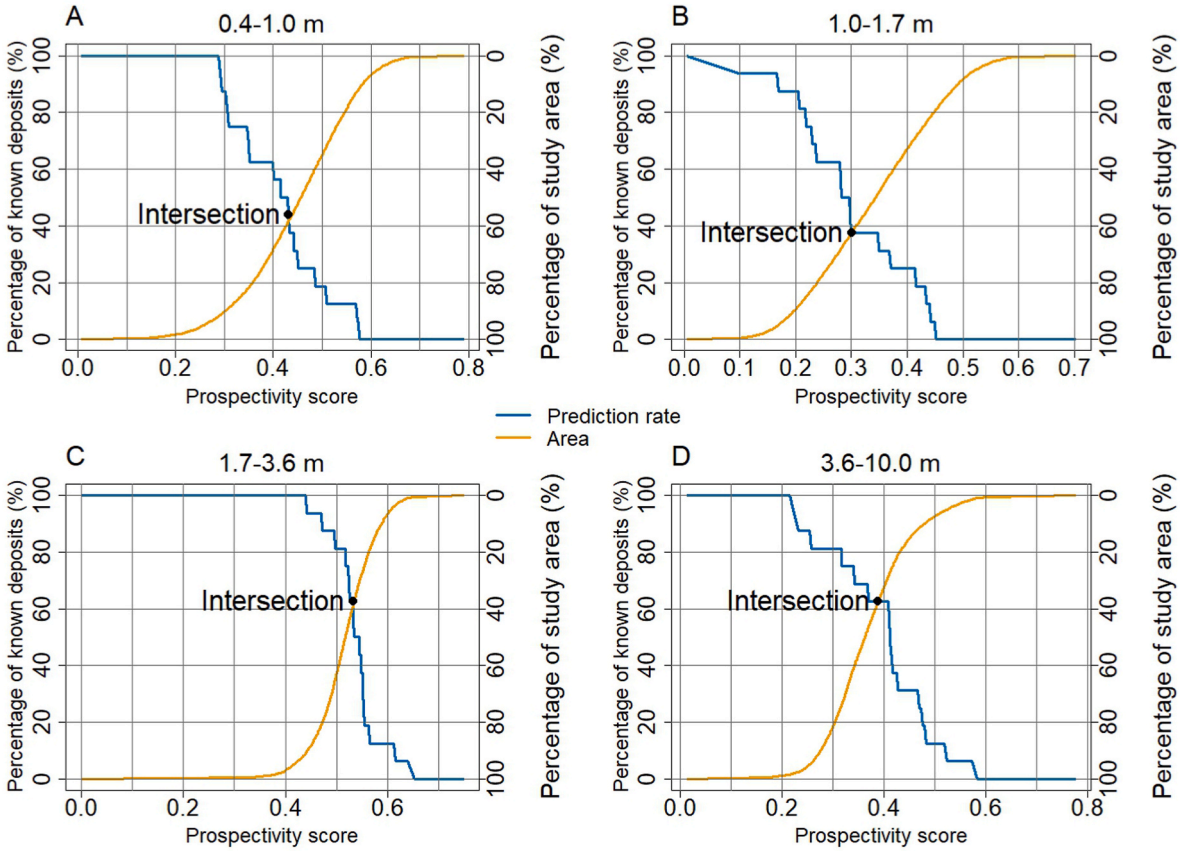


**Fig. 14.** P-A plots for different till depth intervals in study area 1 based on the statistically derived depth-interval method.

**Table 02**
Parameters derived from the intersection points of P–A plots for different depth intervals in study area 1 in Figs. 13 and 14.

| Depth interval | Prediction rate (%) | Proportion of area (%) |
|---|---|---|
| 0–1 m | 50 | 50 |
| 1–2 m | 43 | 57 |
| 2–3 m | 55 | 45 |
| 3–4 m | 58 | 42 |
| 0.4–1.0 m | 42 | 58 |
| 1.0–1.7 m | 38 | 62 |
| 1.7–3.6 m | 62 | 38 |
| 3.6–10.0 m | 62 | 38 |

anomalies effectively represent the known deposits and underlying lithology. In contrast, the results derived from P–A plots show that the 2.8–5.2 m depth interval captures the highest percentage of known mineral deposits (68%) within the smallest percentage of the study area (32%), after excluding the deepest depth interval, 3–4 m. The AUC value related to that interval is 0.6916, which is slightly less than the highest recorded value, 0.7221 that represent 0.5–1.5 m depth interval. However, after taking into account 1) uncertainties associated with randomly selected negative locations used in ROC curves, 2) the fact that the deepest till layers are usually less affected by latest glaciations as the area is located in ice–divide zone where transport distances are very short 3) effects of till transportation on the upper layers; such as till mixing, geochemical signals of the bedrock dilution 4) that the anomalous areas of fuzzy overlay maps for the focused depth intervals (0.5–1.5 m and 2.8–5.2 m) do not show huge differences, it was decided to select the depth interval 2.8–5.2 as the best representative depth interval for orthomagmatic deposits. According to the results by fuzzy maps, AUC values and P–A curves, the best results were obtained from the statistical approach based till profile division method.

The two different favourable ranges of till depth in both study areas may be caused by the nature of the deposits. As an example, when creating the fuzzy overlay maps for gold and orthomagmatic deposits, different elements and different overlaying formulas were used based on the characteristics of deposit types. It is also probable that the difference in favourable ranges is a result of different till transportation dynamics. Referring to the different transport distances as Akanvaara is more towards the southeast (Fig. 1), placing it under the influence of the Salla ice lobe. It means that the glacial transport distances are greater than in the Kittilä area, which has been in the majority under the last ice divide zone. Furthermore, older glacial movements could also have influenced the favourable ranges by eroding and transporting material from variable source areas to be redeposited or mixed into younger tills.

### 5.2. *Possible areas for new mineral deposits using predicted maps*

Study of the anomalies in relation to the geology, indicates some regions with potential for new gold deposits in the Kittilä area. The majority of the known gold deposits are lying on Fe-tholeiitic basalt and theoletiitic basalt rocks nearby or on fracture zones. However, few deposits are associated with mafic graphite tuff and peridotitic komatiite. Within the Kittilä area the favourable areas for gold deposits are associated with areas in proximity to fault structures and high levels of alteration, particularly the albite alteration (Wyche et al., 2015).

In the predicted map concerning 1.7–3.6 m depth interval (Fig. 7C), an anomalous area G-1 is visible on the northeastern corner, underlain by mafic graphite tuff, granodiorite and Fe-tholeiitic basalt rocks. On the western side, the detected anomaly G-2 is following the subadjacent tholeiitic basalt region. Some fractures could be observed within these anomalous regions. Two anomalies, which are primarily located on Fe tholeiitic basalt, gabbro and tholeiitic basalt, mafic graphite tuff are

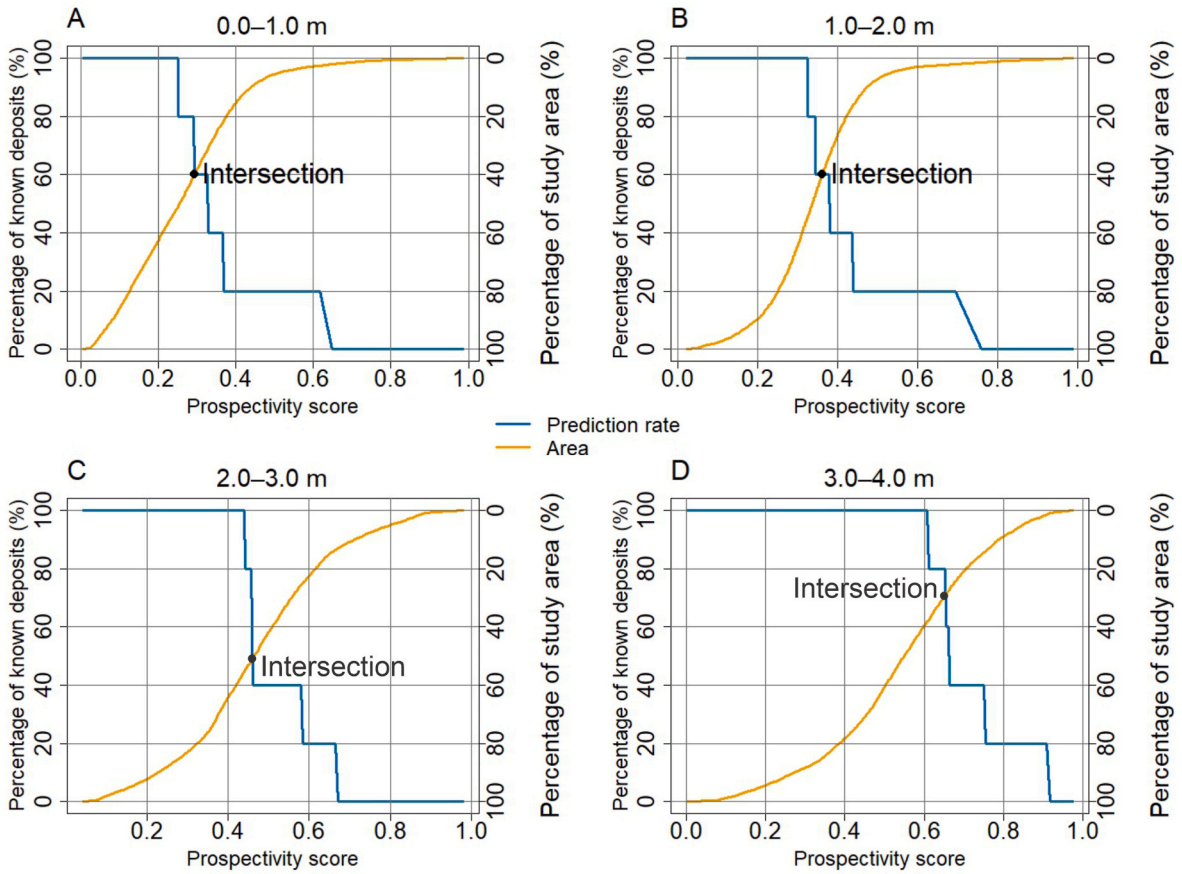


**Fig. 15.** P–A plots for different till depth intervals in study area 2 based on the fixed depth interval method.

visible in the middle eastern side (G-3) and below that area (G-4) respectively. To the east of the Kittilä mine, there is another anomalous area (G-5) on the tholeiitic basalt at the end of a fracture. Furthermore, another two anomalies G-6 and G-7 are underlain by the tholeiitic basalt and mafic graphite tuff, cut by fault structures.

Based on the predicted maps for the Akanvaara area, the most favourable map was obtained for the till depth interval 2.8–5.2 m (Fig. 9C). Apart from the anomalies for the known orthomagmatic deposits, there are other prominent anomalies in the left (O-1), left middle (O-2) and left bottom (O-3) zones of the map (Fig. 9C). The anomalous area O-1 contains komatiite with some minor faults terminating in this region and some nearby faults are also present. The O-2 anomalous area is mainly underlain by peridotitic komatiite whereas banded ironstone, graphite sulfide paraschist also present. The bottom left anomalous zone (O-3) is underlain by komatite, mafic volcanic rock and graphite sulfide paraschist and the anomaly is on the part of a fault structure (GTK, 2024). Apart from those, another anomaly could be observed in the middle (O-4) of the map. The majority of O-4 is underlain by mafic volcanic rock, komatiite and graphite sulfide paraschist.

A widespread magmatic event at 2.5–2.4 Ga emplaced about 20 mafic-ultramafic layered intrusions in the northern Fennoscandian shield and those intrusions host orthomagmatic Ni–Cu-PGE and Cr–V–Ti–Fe deposits (Järvinen et al., 2020). Mafic and ultramafic rocks are favourable for hosting Ni–Cu–Co-PGE sulfide deposits (Moilanen et al., 2019). However, orthomagmatic sulfide deposits are prominent sources for base and precious metals which include Ni, Cu, Co and PGE (Moilanen et al., 2020). Based on the results of studied eight different Ni–Cu-PGE deposits in Finland, the most promising host rocks of those deposits were olivine cumulates, dunite and olivine pyroxenite. According to Konnunaho et al. (2015), komatiites are high-temperature ultramafic lavas which, under favourable conditions could generate Ni–Cu sulfide deposits. Moreover, the most promising host rocks are komatiitic lavas, komatiitic basalts, especially linked to olivine-rich cumulates within lava channels. Sills and feeder dikes linked to komatiitic magmatism can also host Ni–Cu–PGE mineralization. Furthermore, according to their classification into the Finnish komatiite-hosted Ni–Cu-PGE deposits, Lomalampi and Hotinvaara are the related known Paleoproterozoic deposits in the central Lapland belt. However, it is not possible to conclude that all komatiite rocks contain mineralizations. There is a potential to host Ni–Cu-PGE deposits in komatiite of anomalous areas (O-1, O-2, O-3 and O-4), in the selected area.

Considering Fig. 10, the fuzzy overlay maps generated using the regional till dataset do not reveal the known deposits and geology better than the targeting till maps. However, it was found to be a little bit too sparse for many types of mineralized structures and ore deposits in the bedrock. The reason for this difference is the sampling density between two datasets. As expected, the lower resolution sampling reveals the broader zones of known mineralizations quite well but does not provide a detailed visualization as the targeting till dataset. Moreover, when regional till data was used, the overlay map (Fig. 10A) was unable to predict certain known gold mineralizations in the northern region. Nevertheless, it is important to note that we followed the same procedure used in generating the targeting till data fuzzy overlay maps when generating overlay maps for regional till data. Therefore, although additional elements such as Au, Te are available in the regional till dataset, they were not included in the analysis in order to maintain consistency with overlay maps of targeting till data set and allow direct comparison between the two data sets based on sampling density. This article is primarily based on the targeting till data set and the regional till data set was used only to show how the same methodology performs when applied to sparce sampling densities. Moreover, stratigraphical analyses could not be performs on the regional till data set as it contains

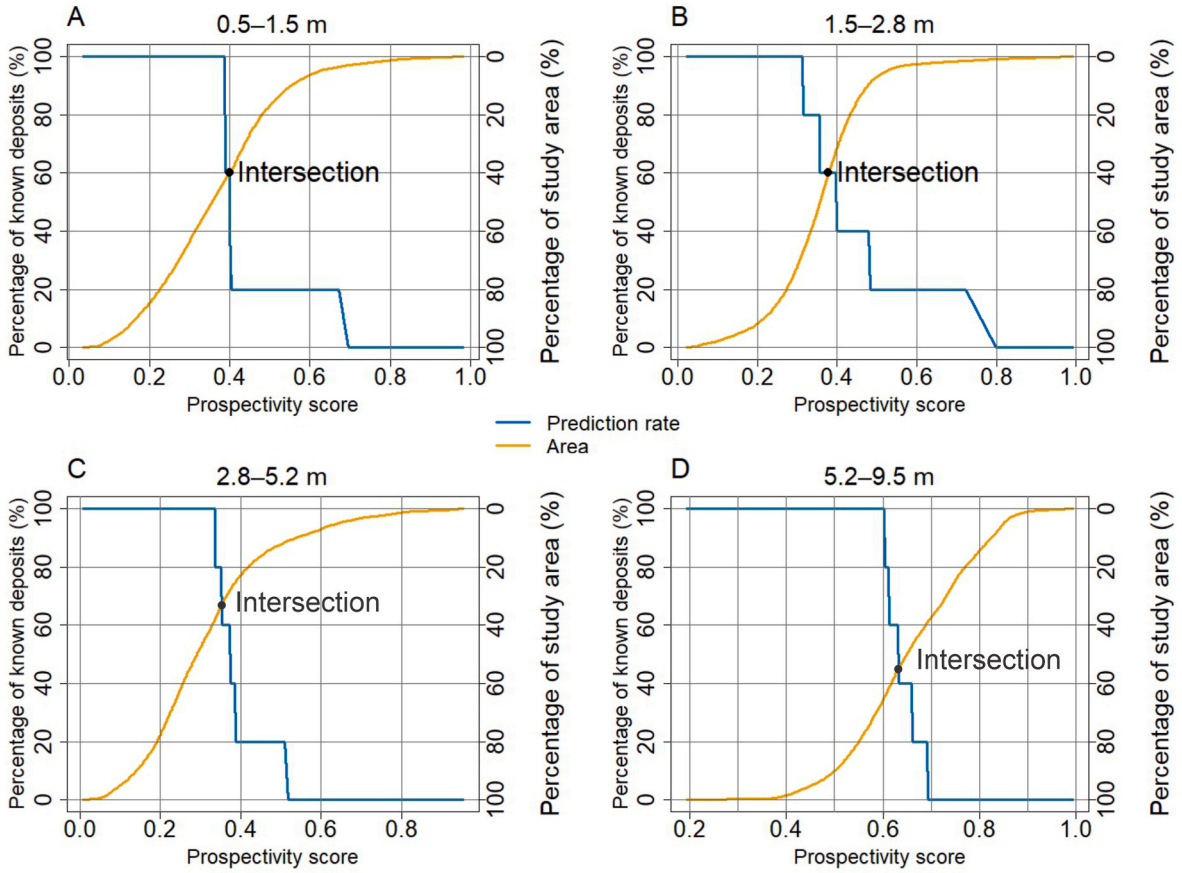


**Fig. 16.** P–A plots for different till depth intervals in study area 2 based on the statistically derived depth-interval method.

**Table 03**
Parameters derived from the intersection points of P–A plots for different depth intervals in study area 2 in Figs. 15 and 16.

| Depth interval | Prediction rate (%) | Area (%) |
|---|---|---|
| 0–1 m | 60 | 40 |
| 1–2 m | 60 | 40 |
| 2–3 m | 50 | 50 |
| 3–4 m | 70 | 30 |
| 0.5–1.5 m | 60 | 40 |
| 1.5–2.8 m | 60 | 40 |
| 2.8–5.2 m | 68 | 32 |
| 5.2–9.5 m | 45 | 55 |

concentrations related to a constant 1.5–2 m depth range.

The resultant maps obtained from regional till data might be able to be improved by incorporating other available elements in the dataset, but absent from the targeting till data set. In Fig. 10B (which approximately represents the same depth range as Fig. 9B), areas surrounding the known mineral deposits show high anomaly values, whereas the values diminish towards the eastern part of the map, which is the ice-flow direction of the area. In addition, the relatively coarse sampling grid of the regional till data set may lead to an overestimated anomalous region. Thus, the sampling density of the datasets plays an important role in the visualization of fuzzy overlay maps. Targeting till dataset is a high-resolution dataset where the sampling density is 6-12 samples per $km^2$ and the regional till dataset has a sampling density of 4 samples per $km^2$ (Gustavsson et al., 1979; Salminen, 1995). Reimann et al. (2016) stated that small individual mineral bodies have the potential to be undiscovered when low sampling densities are used. They also mentioned that using low sampling density would be advantageous to identify mineral systems, including geology, processes needed for generating targeted mineral deposits during the early stages of mineral exploration.

## 6. Conclusion

In the glaciated terrains, till geochemical data have been collected since 1960's, and many large datasets are available from different countries. However, the comparison of datasets from different decades can be challenging due to differences between sampling and sample processing techniques, analytical methods and the list of analysed elements. Consideration of those variable parameters typically requires data corrections, cleaning and levelling before using the data. In addition, geochemical data should be considered as compositional data and statistically handled accordingly. However, even old geochemical datasets can be useable and provide an environmentally friendly way to do mineral exploration as a part of statistical data analysis and prospectivity modelling.

We demonstrate the data cleaning and statistical analysis techniques for the old till geochemical dataset collected during the 1970s and early 1980s from northern Finland. This so-called targeting till geochemical dataset was sampled using percussion drilling with a density of 6–12 samples per $km^2$ and by following lines with a 100–400 m interval. From the till samples, the sieved <0.06 mm size fraction was used to be analysed using an emission quantometer analyser. A Total of 17 elements were analysed, of which after quality control, certain indicator elements were chosen to identify till beds and the most suitable layers for the mineral exploration of Au and the orthomagmatic related metal mineralizations in two study areas in northern Finland. The results show that the statistical method for determining optimal till depth for locating mineral deposits is more favourable and reliable compared to fixed depth intervals. It can be seen based on higher AUC values for both Au

and orthomagmatic mineralization examples and from related P–A plots as well. To analyse data and detect till depth intervals, it is suggested to clean and level the data beforehand, considering the coverage and quality of the datasets. Case studies in northern Finland show that the optimal till depth interval for detecting gold deposits in the Kittilä area is 1.7–3.6 m, whereas for orthomagmatic deposits in the Akanvaara area, it is 2.8–5.2 m, consistent with till bed III. Additionally, when applying the ROC method to validate results, it is recommended to also consider geological factors, as the AUC values can be misleading when the number of positive and negative points is low.

Sampling density plays an important role in generating predicted maps. During the early stages of mineral exploration, a low sampling density dataset like regional till would be beneficial to outline favourable regions for targeted mineral deposits. Nevertheless, high-resolution datasets such as targeting till dataset are more effective for identifying mineral deposits, even having a small suboutcrop. For example, in this research, the zones G-1 to G-7 in the Kittilä area at till depth interval 1.7–3.6 m and the zones O-1 to O-4 in the Akanvaara area at till depth range between 2.8 and 5.2 m are recognized as the most favourable targets for new prospective gold and orthomagmatic mineral deposits.

Future works: As archived sample material exists, a modern reanalysis would be possible and could open up a whole new suite of elements for exploration and detailed research in the area.

## CRediT authorship contribution statement

**C. Kalubowila:** Conceptualization, Data curation, Formal analysis, Methodology, Visualization, Writing – original draft. **M. Raatikainen:** Conceptualization, Data curation, Formal analysis, Methodology, Visualization, Writing – original draft. **P. Sarala:** Conceptualization, Methodology, Supervision, Writing – review & editing.

## Declaration of competing interest

The authors declare the following financial interests/personal relationships which may be considered as potential competing interests: Charmee Kalubowila reports financial support was provided by Horizon Europe (SEMACRET, Grant Agreement no. 101057741). Charmee Kalubowila reports financial support was provided by K H Renlund Foundation. Markus Raatikainen reports financial support was provided by K H Renlund Foundation. Markus Raatikainen reports financial support was provided by University of Oulu. Pertti Sarala reports equipment, drugs, or supplies was provided by Geological Survey of Finland. Charmee Kalubowila reports a relationship with University of Oulu that includes: employment. Markus Raatikainen reports a relationship with University of Oulu that includes: employment. Pertti Sarala reports a relationship with University of Oulu that includes: employment. If there are other authors, they declare that they have no known competing financial interests or personal relationships that could have appeared to influence the work reported in this paper.

## Acknowledgements

This work was co-funded by Horizon Europe (SEMACRET, Grant Agreement no. 101057741), K. H. Renlund Foundation, and the University of Oulu. We thank the Geological Survey of Finland for open access geochemical datasets that were used in this study. In addition, the authors gratefully acknowledge Malcom Aranha for his feedback on the prediction maps created in this study. Special thanks go also to Dr. Roger Paulen and two anonymous reviewers and the Associate Editor Oliver Kreuzer of Applied Geochemistry for constructive criticism and proposals for corrections, which improved the manuscript.

## Appendices.

**Table A1**
Summary table of element concentration ranges in till, sampling density, and total number of data points by depth intervals.

| | Depth (m) | Total points | Point density (n/km$^2$) | Concentration (ppm) | | | | | | | | |
|---|---|---|---|---|---|---|---|---|---|---|---|---|
| | | | | Ca | Co | Cr | Cu | Fe | Mg | Ni | Ti | V |
| Gold maps | 0.0-1.0 | 5853 | 2.076 | 320-70200 | 1.24-148 | 2.39-3620 | 0.96-2850 | 154-314000 | 1190-230000 | 2.27-3630.1 | 1050-19400 | 7.95-950 |
| | 1.0-2.0 | 11797 | 4.183 | 47.8-72400 | 1.675-184 | 2.39-5670.1 | 0.4465-8470.1 | 154-1181000 | 119.5-118000 | 0.422-3240.1 | 500-19700 | 12.9-998 |
| | 2.0-3.0 | 3038 | 1.077 | 47.8-128000 | 1.24-170 | 2.39-4160 | 0.53-5900.1 | 154-356000 | 2020-110000 | 1.165-2850 | 500-15300 | 23.05-980 |
| | 3.0-4.0 | 1565 | 0.555 | 456.5 - 223000 | 1.79-160 | 3.315 - 1700 | 2.70 - 1850 | 154 - 324000 | 4010 - 77500 | 2.43 - 2770 | 1370 - 14700 | 21.8 - 947 |
| | 0.4-1.0 | 6677 | 2.395 | 320-70200 | 1.24-148 | 2.39-3620 | 0.96-2850 | 154-314000 | 1190-230000 | 2.27-3630.1 | 1050-19400 | 7.95-950 |
| | 1.0-1.7 | 5389 | 1.923 | 47.8-61300 | 1.675-184 | 3.755-5670.1 | 0.665-1280 | 154-361000 | 1420-91800 | 2.095-3240.1 | 500-17600 | 12.9-998 |
| | 1.7-3.6 | 10917 | 3.887 | 47.8-128000 | 1.24-170 | 2.39-4770 | 0.4465-8470.1 | 154-1181000 | 119.5-118000 | 0.422-2850 | 500-19700 | 13.6-980 |
| | 3.6-10 | 2834 | 1.007 | 423.5-842000 | 2.245-146 | 2.39-2360 | 2.12-1850 | 154-318000 | 1370-80800 | 4.35-1840 | 1440-14700 | 29.3-969 |
| Orthomagmatic maps | 0.0-1.0 | 1617 | 2.073 | 1200-376500 | 4.34-121 | 4.6-8595 | 0.695-3450 | 1090-541500 | 218-130000 | 0.459-5325 | 1000-21400 | 6.66-2955 |
| | 1.0-2.0 | 4616 | 5.916 | 1620-202000 | 1.34-170 | 7.7-10470 | 3.13-4710 | 2030-537000 | 1150-129000 | 8.81-6705 | 500-24700 | 12.8-3000 |
| | 2.0-3.0 | 1220 | 1.564 | 1240-148000 | 6.85-160 | 46.7-9195 | 2.34-4900 | 7430-540000 | 4230-129000 | 14.8-5745 | 1080-24700 | 28.5-1210 |
| | 3.0-4.0 | 651 | 0.834 | 2010-161000 | 12.3-76.9 | 86.3-11355 | 2.83-1860 | 4940-208000 | 5120-114000 | 31.2-2930 | 1230-24700 | 33.3-1410 |
| | 0.5-1.5 | 2537 | 3.252 | 1200-376500 | 1.34-152 | 4.6-8595 | 0.695-3450 | 1090-541500 | 218-130000 | 0.459-5325 | 820-23500 | 9.72-2955 |

(*continued on next page*)

**Table A1** (*continued*)

| | Depth (m) | Total points | Point density (n/km$^2$) | Concentration (ppm) | | | | | | | | |
|---|---|---|---|---|---|---|---|---|---|---|---|---|
| | | | | Ca | Co | Cr | Cu | Fe | Mg | Ni | Ti | V |
| | 1.5-2.8 | 4070 | 5.216 | 1240-202000 | 3.31-170 | 9.24-10470 | 3.13-4900 | 5000-540000 | 4230-129000 | 14.8-6705 | 500-24700 | 13.4-3000 |
| | 2.8-5.2 | 1791 | 2.296 | 2010-161000 | 9.16-102 | 60-11355 | 2.34-1860 | 4940-248000 | 5120-129000 | 26.3-6525 | 1230-24700 | 33.3-1410 |
| | 5.2-9.5 | 389 | 0.498 | 0.638-5.22 | 12.4-62.7 | 133-4080 | 3.25-1750 | 12400-236000 | 9900-106000 | 66.8-2490 | 3020-12000 | 121-1130 |

## Data availability

The authors do not have permission to share data.

## References


Aho, P., 2009. Malmimineraloginen Ja Geokemiallinen Vaihtelu Kahdella Suurikuusikon Kultakaivosalueen Tutkimusprofiililla. M.Sc. thesis, University of Oulu, p. 91 (in Finnish).

Ahtonen, N., Hölttä, P., Huhma, H., 2007. Intracratonic Palaeoproterozoic granitoids in northern Finland. Prolonged and episodic crustal melting events revealed by Nd isotopes and U-Pb ages on zircon. Bull. Geol. Soc. Finland 79, 143–174. https://doi.org/10.17741/bgsf/79.2.002.

Aitchison, J., 1982. The statistical analysis of compositional data (with discussion). J. R. Stat. Soc., Ser. B Stat. Methodol. 44, 139–177.

Aitchison, J., 1983. Principal component analysis of compositional data. Biometrika 70, 57–65.

Aitchison, J., 1986. The Statistical Analysis of Compositional Data. The Blackburn Press. Chapman and Hall, London, Reprinted in 2003 with additional material by.

Bonham-Carter, G.F., 1994. Geographic Information Systems for Geoscientists. Elsevier. Modelling with GIS.

Chernet, T., Kojonen, K., Pakkanen, L., 2000. Applied mineralogical study on the near-surface Suurikuusikko refractory gold ore. Kittilä, Western Finnish Lapland (Phase 1). Geological Survey of Finland Report C/MA9/2743/2000/10, p. 22.

Daneshfar, B., Cameron, E., 1998. Levelling geochemical data between map sheets. J. Geochem. Explor. 63, 189–201. https://doi.org/10.1016/S0375-6742(98)00015-6.

Danielsson, A., Lundgren, F., Sundkvist, G., 1959. The tape machine – I: a new tool for spectrochemical analysis. Spectrochim. Acta 15, 122–125. https://doi.org/10.1016/S0371-1951(59)80296-4.

Danielsson, A., Sundkvist, G., 1959a. The tape machine – II: applications using different kinds of isoformations. Spectrochim. Acta 15, 126–133. https://doi.org/10.1016/S0371-1951(59)80297-6.

Danielsson, A., Sundkvist, G., 1959b. The tape machine – III: notes on useful corrections in spectrochemical analysis with the tape technique. Spectrochim. Acta 15, 134–137. https://doi.org/10.1016/S0371-1951(59)80298-8.

Ehlers, J., Gibbard, P.L., 2007. The extent and chronology of Cenozoic global glaciation. Quat. Int. 16–20. https://doi.org/10.1016/j.quaint.2006.10.008.

Eilu, P., Pankka, H., Keinänen, V., Kortelainen, V., Niiranen, T., Pulkkinen, E., 2007. Characteristics of gold mineralisation in the greenstone belts of Northern Finland. Geol. Surv. Finland, Special Paper 44, 57–106.

Fišerová, E., Hron, K., 2011. On interpretation of orthonormal coordinates for compositional data. Math. Geosci. 43, 455–468. https://doi.org/10.1007/s11004-011-9333-x.

Filzmoser, P., Hron, K., Templ, M., 2018. Principal component analysis. In: Applied Compositional Data Analysis. with Worked Examples in R. Springer International Publishing, Cham, pp. 131–148.

Geological Survey of Finland, 2015. Spatial Data Products: Targeting till Geochemistry. Geological Survey of Finland [Data set]. https://hakku.gtk.fi/en/locations?orderBy=nameEn&search=till+&submit=true. (Accessed 1 August 2022).

GTK, 2024. Till geochemistry sample series. https://tupa.gtk.fi/paikkatieto/meta/targeting_till_geochemistry.html.

Gustavsson, N., Lampio, E., Nilsson, B., Norblad, G., Ros, F., Salminen, R., 1994. Geochemical maps of Finland and Sweden. J. Geochem. Explor. 51, 143–160. https://doi.org/10.1016/0375-6742(94)90015-9.

Gustavsson, N., Noras, P., Tanskanen, H., 1979. Seloste geokemiallisen kartoituksen tutkimusmenetelmistä. Geol. Surv. Finland, Rep. Invest. 39, 1–20.

Hansen, H., Slagstad, T., Bergh, S.G., Bekker, A., 2023. Geochronology and chemostratigraphy of the 2.47–1.96 Ga rift-related volcano-sedimentary succession in the Karasjok Greenstone Belt, northern Norway, and its regional correlation within the fennoscandian Shield: precam. Res. 397, 107166. https://doi.org/10.1016/j.precamres.2023.107166.

Hanski, E., Huhma, H., 2005. Central Lapland greenstone belt. Dev. Precambrian Geol. 14, 139–193. Elsevier.

Hirvas, H., 1991. Pleistocene stratigraphy of Finnish Lapland. Geol. Surv. Finland. Bulletin 354, 123.

Hölttä, P., Väisänen, M., Väänänen, J., Manninen, T., 2007. Paleoproterozoic metamorphism and deformation in central Lapland, Finland: Geol. Surv. Finland, Special Paper 44, 7–56.

Härkönen, I., 1997. Tutkimustyöselostus Kittilän Kunnassa Valtausalueilla Suurikuusikko 2 Ja Rouravaara 1–10 (Kaivosrekisterinumerot 5965/1, 6160/1, 6288/1–6288/9) Suoritetuista Kultatutkimuksista Vuosina 1987–1997: Geol. Surv. Finland, Report M 06/2743/97/1, 47 pp. (in Finnish).

Härkönen, I., Pankka, H., Rossi, S., 2000. Summary Report: the Iso-Kuotko Gold Prospects, northern Finland Kuorko 8-10 (6314/1-3) and Kuotko 11-13 (6886/1-3). Geological Survey of Finland. Claim report, 21.

Hughes, H.S., Andersen, J.C., O'Driscoll, B., 2021. Mineralization in layered mafic-ultramafic intrusions. In: Alderton, D., Elias, S.A. (Eds.), Encyclopedia of Geology, second ed. Academic Press, Amsterdam, pp. 823–839. https://doi.org/10.1016/B978-0-08-102908-4.00037-0.

Hulkki, H., Keinänen, V., 2007. The alteration and fluid inclusion characteristics of the hirvilavanmaa gold deposit, central Lapland greenstone Belt, Finland. Geol. Surv. Finland, Spec. Pap. 44, 137–153.

Höytiä, H.M., Jelsma, H.A., Armstrong, R.A., Dodds, P., Siikaluoma, J., Lamberg, P., 2024. SHRIMP U-Pb geochronology of the Sakatti and Kaarrekumpu Cu-Ni-Platinum Group element Deposits—Constraints on the timing of fertile magmatism in the central Lapland greenstone Belt. Econ. Geol. 119, 1769–1790. https://doi.org/10.5382/econgeo.5112.

Hyyppä, J., 1983. Suomen kallioperän preglasiaalisesta rapautumisesta, summary: preglacial weathering of Precambrian rocks in Finland. Geol. Soc. Finland, Papers Engin. 15, 1–17. Available at: https://tupa.gtk.fi/raportti/arkisto/p13_5_3_019.pdf.

Johansson, P., Lunkka, J.P., Sarala, P., 2011. The glaciation of Finland. In: Ehlers, J., Gibbard, P.L., Hughes, P.D. (Eds.), Developments in Quaternary Science, vol. 15. Elsevier, Amsterdam, pp. 105–116. https://doi.org/10.1016/B978-0-444-53447-7.00009-X.

Johansson, P., Kujansuu, R., 2005. Pohjois-Suomen Maaperä: Maaperäkarttojen 1:400 000 Selitys. Summary: Quaternary Deposits of Northern Finland - Explanation to the Maps of Quaternary Deposits 1:400 000: Geol. Surv. Finland.

Järvinen, V., Halkoaho, T., Konnunaho, J., Heinonen, J.S., Rämö, O.T., 2020. Parental magma, magmatic stratigraphy, and reef-type PGE enrichment of the 2.44-Ga mafic-ultramafic Näränkävaara layered intrusion, Northern Finland: mineral. Depo 55 (8), 1535–1560. https://doi.org/10.1007/s00126-019-00934-z.

Kalubowila, C., Sarala, P., Pospiech, S., Filzmoser, P., 2025. Exploring high-resolution targeting till geochemical data in central Lapland, Finland. Bull. Geol. Soc. Finland 97, 65–84. https://doi.org/10.17741/bgsf/97.1.003.

Killick, R., Eckley, I.A., 2014. Changepoint: an R package for changepoint analysis. J. Stat. Software 58, 1–19. https://doi.org/10.18637/jss.v058.i03.

Kojonen, K., Johanson, B., 1999. Determination of refractory gold distribution by microanalysis, diagnostic leaching and image analysis. Mineral. Petrol. 67, 1–19. https://doi.org/10.1007/BF01165112.

Konnunaho, J., Halkoaho, T., Hanski, E., Törmänen, T., 2015. Komatiite-hosted Ni-Cu-PGE deposits in Finland. In: Mayer, W.D., Lahtinen, R., O'Brien, H. (Eds.), Mineral Deposits of Finland. Elsevier, Amsterdam, pp. 93–131. https://doi.org/10.1016/B978-0-12-410438-9.00004-2. Chapter 3.2.

Köykkä, J., Lahtinen, R., Huhma, H., 2019. Provenance evolution of the Paleoproterozoic metasedimentary cover sequences in northern Fennoscandia: age distribution, geochemistry, and zircon morphology. Precambr. Res. 331, 105364. https://doi.org/10.1016/j.precamres.2019.105364.

Köykkä, J., Luukas, J., 2021. Keski-Lapin Litostratigrafia Ja Paleoproterotsooisen Sodankylän Ryhmän Kivilajiyksiköiden Määrittely, Summary: Lithostratigraphy of the Central Lapland Area and Definition of the Paleoproterozoic Sodankylä Group Rock Units, 13/2021. Geological Survey of Finland, Open File Research Report. Available at: https://tupa.gtk.fi/raportti/arkisto/13_2021.pdf.

Lehtonen, M., Airo, M.-L., Eilu, P., 1998. Kittilän vihreäkivialueen geologia. Summary: the stratigraphy, petrology and geochemistry of the Kittilä greenstone area, northern Finland. Geol. Surv. Finland, Rep. Invest. 140.

Lindgren, A., Hugelius, G., Kuhry, P., Christensen, T.R., Vandenberghe, J., 2016. GIS-based maps and area estimates of Northern Hemisphere permafrost extent during the last Glacial Maximum. Permafr. Periglac. Process. 27, 6–16. https://doi.org/10.1002/ppp.1851.

Lunkka, J.P., Sarala, P., Gibbard, P.L., 2015. The Rautuvaara stratotype section, western Finnish Lapland revisited – new age constraints on the sequence indicate complex Scandinavian Ice Sheet history in northern Fennoscandia during the Weichselian Stage. Boreas 44, 68–80. https://doi.org/10.1111/bor.12088.

Luolavirta, K., Hanski, E., Maier, W., Santaguida, F., 2018. Whole-rock and mineral compositional constraints on the magmatic evolution of the Ni-Cu-(PGE) sulfide ore-bearing Kevitsa intrusion, northern Finland. Lithos 296, 37–53. https://doi.org/10.1016/j.lithos.2017.10.015.

Maier, W.D., Lahtinen, R., O'Brien, H., 2015. Mineral Deposits of Finland. Elsevier, Amsterdam, p. 819.

Maier, W.D., Hanski, E.J., 2017. Layered mafic–ultramafic intrusions of fennoscandia: Europe's treasure chest of magmatic metal deposits. Elements 13, 415–420. https://doi.org/10.2138/gselements.13.6.415.

Main, P.T., Champion, D.C., 2022. Levelling of multi-generational and spatially isolated geochemical surveys. J. Geochem. Explor. 240, 107028. https://doi.org/10.1016/j.gexplo.2022.107028.

Manninen, T., 1991. Sallan alueen vulkaniitit: lapin vulkaniittiprojektin raportti. Summary: volcanic rocks in the Salla area, northeastern Finland: a report of the Lapland Volcanite Project. Geol. Surv. Finland, Rep. Invest. 104, 97.

McClenaghan, M.B., Paulen, R.C., Smith, I.R., Rice, J.M., Plouffe, A., McMartin, I., Campbell, J.E., Lehtonen, M., Parsasadr, M., Beckett-Brown, C.E., 2023. Review of till geochemistry and indicator mineral methods for mineral exploration in glaciated terrain. Geochem. Explor. Environ. Anal. 23 (4). https://doi.org/10.1144/geochem2023-013 geochem2023-013.

McClenaghan, M.B., Paulen, R.C., 2018. Application of till mineralogy and geochemistry to mineral exploration. In: Menzies, J., van der Meer, J.J.M. (Eds.), Past Glacial Environments, second ed. Elsevier, Amsterdam, pp. 689–751. https://doi.org/10.1016/B978-0-08-100524-8.00022-1.

Mäkinen, K., 1975. Maapeitteen Paksuudesta Keski-Lapissa. M.Sc. Thesis. The University of Turku, Turku, Finland, p. 70.

Moilanen, M., Hanski, E., Konnunaho, J., Törmänen, T., Yang, S.H., Lahaye, Y., et al., 2020. Composition of iron oxides in Archean and Paleoproterozoic mafic-ultramafic hosted Ni-Cu-PGE deposits in northern Fennoscandia: application to mineral exploration. Miner. Depos. 55, 1515–1534. https://doi.org/10.1007/s00126-020-00953-1.

Moilanen, M., Hanski, E., Konnunaho, J., Yang, S.H., Törmänen, T., Li, C., Zhou, L.M., 2019. Re-Os isotope geochemistry of komatiite-hosted Ni-Cu-PGE deposits in Finland. Ore Geol. Rev. 105, 102–122. https://doi.org/10.1016/j.oregeorev.2018.12.007.

Mutanen, T., 1997. Geology and petrology of the Akanvaara and Koitelainen mafic layered intrusions and the Keivitsa-Satovaara layered complex, Northeastern Finland. Geol. Surv. Finland 395. Bulletin.

Niiranen, T., Nykänen, V., Lahti, I., 2019. Scalability of the mineral prospectivity modelling – an orogenic gold case study from northern Finland. Ore Geol. Rev. 109, 11–25. https://doi.org/10.1016/j.oregeorev.2019.04.002.

Nykänen, V., Lahti, I., Niiranen, T., Korhonen, K., 2015. Receiver Operating Characteristics (ROC) as validation tool for prospectivity models e a magmatic Ni-Cu case study from the Central Lapland greenstone belt, Northern Finland. Ore Geol. Rev. 71, 853–860. https://doi.org/10.1016/j.oregeorev.2014.09.007.

Obuchowski, N.A., 2003. Receiver operating characteristic curves and their use in radiology. Radiology 229, 3–8. https://doi.org/10.1148/radiol.2291010898.

Patison, N.L., 2007. Structural controls on gold mineralisation in the Central Lapland Greenstone Belt. Geol. Surv. Finland, Special Paper 44, 107–124.

Patison, N.L., Salamis, G., Kortelainen, V.J., 2007. The Suurikuusikko gold deposit. Project development summary of northern Europe's largest gold resource. Geol. Surv. Finland, Special Paper 44, 125–136.

Patten, C.G.C., Molnár, F., Pitcairn, I.K., Kolb, J., Mertanen, S., Hector, S., 2023. Multi-source and multi-stage metal mobilization during the tectonic evolution of the Central Lapland Greenstone Belt, Finland: implications for the formation of orogenic Au deposits. Miner. Depos. 58, 461–488. https://doi.org/10.1007/s00126-022-01133-z.

Pawlowsky-Glahn, V., Egozcue, J.J., 2001. Geometric approach to statistical analysis on the simplex. Stoch. Environ. Res. Risk Assess. 15, 384–398. https://doi.org/10.1007/s004770100077.

Pereira, B., Vandeuren, A., Govaerts, B.B., Sonnet, P., 2016. Assessing dataset equivalence and leveling data in geochemical mapping. J. Geochem. Explor. 168, 36–48. https://doi.org/10.1016/j.gexplo.2016.05.012.

Pereira, B., Vandeuren, A., Sonnet, P., 2015. Geochemical mapping based on multiple geochemical datasets: a general method, and its application to Wallonia (Southern Belgium). J. Geochem. Explor. 158, 34–43. https://doi.org/10.1016/j.gexplo.2015.06.016.

Puchhammer, P., Kalubowila, C., Braus, L., Pospiech, S., Sarala, P., Filzmoser, P., 2024. A performance study of local outlier detection methods for mineral exploration with geochemical compositional data. J. Geochem. Explor. 258, 107392.

Putkinen, N., Sarala, P., Eyles, N., Daxberger, H., Pihlaja, J., Murray, A., 2020. Reworked Middle Pleistocene deposits preserved in the core region of the Fennoscandian Ice Sheet. Quat. Sci. Adv. 2, 100005. https://doi.org/10.1016/j.qsa.2020.100005.

R Core Team, 2022. R: a Language and Environment for Statistical Computing. R Foundation for Statistical Computing, Vienna, Austria. Retrieved February 10, 2025, from. https://www.R-project.org.

Raatikainen, M., Sarala, P., Ranta, J.-P., 2025. Self-organizing map modelling and prospectivity mapping of surface geochemical data in Au and multi-metal mineral exploration: example from northern Finland. Geochem. Explor. Environ. Anal. 25. https://doi.org/10.1144/geochem2024-055 geochem2024-055.

Rajamani, V., Naldrett, A.J., 1978. Partitioning of Fe, Co, Ni, and Cu between sulfide liquid and basaltic melts and the composition of Ni-Cu sulfide deposits. Econ. Geol. 73 (1), 82–93. https://doi.org/10.2113/gsecongeo.73.1.82.

Rasilainen, K., Eilu, P., Äikäs, O., Halkoaho, T., Heino, T., Iljina, M., Törmänen, T.O., 2012. Quantitative mineral resource assessment of nickel, copper and cobalt in undiscovered Ni-Cu deposits in Finland. Geol. Surv.Finland, Rep.Invest. 194, 514.

Rasilainen, K., Eilu, P., Halkoaho, T., Iljina, M., Karinen, T., 2010. Quantitative mineral resource assessment of platinum, palladium, gold, nickel, and copper in undiscovered PGE deposits in mafic-ultramafic layered intrusions in Finland. Geol. Surv.Finland, Rep.Invest. 180, 338.

Reimann, C., Filzmoser, P., Fabian, K., Hron, K., Birke, M., Demetriades, A., GEMAS Project Team, 2012. The concept of compositional data analysis in practice – total major element concentrations in agricultural and grazing land soils of Europe. Sci. Tot. Envi. 426, 196–210. https://doi.org/10.1016/j.Scitotenv.2012.02.032.

Reimann, C., Ladenberger, A., Birke, M., Caritat, P.D., 2016. Low density geochemical mapping and mineral exploration: application of the mineral system concept. Geochem. Explor. Environ. Anal. 16, 48–61. https://doi.org/10.1144/geochem2014-327.

Roshanravan, B., Aghajani, H., Yousefi, M., Kreuzer, O., 2019. An improved prediction-area plot for prospectivity analysis of mineral deposits. Nat. Resour. Res. 28 (3), 1089–1105. https://doi.org/10.1007/s11053-018-9439-7.

Salminen, R., Ed., 1995. Alueellinen Geokemiallinen Kartoitus Suomessa Vuosina 1982-1994, Summary: Regional Geochemical Mapping in Finland in 1982-1994. Geol. Surv. Finland, Rep. of invest. vol. 130, 47 p.

Salminen, R., Tarvainen, T., 1995. Geochemical mapping and databases in Finland. J. Geochem. Explor. 55, 321–327. https://doi.org/10.1016/0375-6742(94)00062-X.

Saloranta, J., 2011. Albite Alteration at Suurikuusikko, Northern Finland, and its Relation to Gold Deposition. M.Sc. thesis, Univ, Helsinki, p. 95.

Sarala, P., 2011. Stop 2: naakenavaara interglacial deposit in Kittilä. In: Johansson, P., Lunkka, J.-P., Sarala, P. (Eds.), Late Pleistocene Glacigenic Deposits from the Central Part of the Scandinavian Ice Sheet to Younger Dryas End Moraine Zone. Excursion Guide and Abstracts of the INQUA Peribaltic Working Group Meeting and Excursion in Finland, 12-17 June 2011. Geol. Surv. Finland, pp. 13–15.

Sarala, P., 2014. OSL Dating of the Inter-till Stratified Sediments of the Naakenavaara Key Section in Kittilä, Northern Finland, vol 2014. 31st Nordic Geological Winter Meeting, Lund, Sweden.

Sarala, P., 2015. Surficial geochemical exploration methods. In: Mayer, W.D., Lahtinen, R., O'Brien, H. (Eds.), Mineral Deposits of Finland. Elsevier, Amsterdam, pp. 711–731. https://doi.org/10.1016/B978-0-12-410438-9.00027-3. Chapter 10.1.

Sarala, P., Nykänen, V., 2017. Spatial analysis and modelling of glaciogenic geochemical dispersion – implication for mineral exploration in Finland. J. Afr. Earth Sci. 128, 61–71. https://doi.org/10.1016/j.jafrearsci.2016.12.002.

Shilts, W.W., 1976. Glacial till and mineral exploration. Glacial Till, Interdiscipl. Stud. 12, 205–223. Royal Society of Canada, Special Publication.

S&P global market intelligence, 2024. 2024. corporate Exploration strategies. https://www.spglobal.com/market-intelligence/en/events/webinars/2024-corporate-exploration-strategies.

Taivalkoski, A., 2017. Vanhojen moreenigeokemian analyysiaineistojen käytettävyyden arviointi - Itä-Lapin uusinta-analyyseihin perustuva vertailututkimus. Msc Thesis, Oulu Mining School. University of Oulu, p. 51. In Finnish. http://urn.fi/URN:NBN:fi:oulu-860201709052793.

Tsoukalas, L.H., Uhrig, R.E., 1997. Fuzzy and Neural Approaches in Engineering. J. Wiley and Sons, New York, p. 608.

Williams, P.M., 2021. Statistical levelling of multi-element geochemical data. Appl. Comp.Geosci. 10, 1–14. https://doi.org/10.1016/j.acags.2021.100060.

Wyche, N.L., Eilu, P., Koppström, K., Kortelainen, V.J., Niiranen, T., Välimaa, J., 2015. The suurikuusikko gold deposit (Kittilä mine), Northern Finland. In: Mayer, W.D., Lahtinen, R., O'Brien, H. (Eds.), Mineral Deposits of Finland. Elsevier, Amsterdam, pp. 411–433. https://doi.org/10.1016/b978-0-12-410438-9.00016-9. Chapter 5.2.

Yousefi, M., Carranza, E.J.M., 2015a. Prediction–area (P–A) plot and C–A fractal analysis to classify and evaluate evidential maps for mineral prospectivity modeling. Comput. Geosci. 79, 69–81. https://doi.org/10.1016/j.cageo.2015.03.0.

Yousefi, M., Carranza, E.J.M., 2015b. Fuzzification of continuous-value spatial evidence for mineral prospectivity mapping. Comput. Geosci. 74, 97–109. https://doi.org/10.1016/j.cageo.2014.10.014.

Zadeh, L.A., 1965. Fuzzy sets. Inf. Control 8, 338–353.

Zimmermann, H.-J., Zysno, P., 1980. Latent connectives in human decision making. Fuzzy Set Syst. 4, 37–51. https://doi.org/10.1016/0165-0114(80)90062-7.